Tectonophysics 667 (2016) 144–162

Contents lists available at ScienceDirect

Tectonophysics

journal homepage: www.elsevier.com/locate/tecto

Tectonic styles and crustal shortening of the Central Andes "Pampean" flat-slab segment in northern Chile (27–29°S)

Fernando Martínez [a,*], César Arriagada [a], Matías Peña [a], Katja Deckart [a,c], Reynaldo Charrier [a,b,c]

[a] Departamento de Geología, Facultad de Ciencias Físicas y Matemáticas, Universidad de Chile, Santiago, Chile
[b] Escuela de Ciencias de la Tierra, Universidad Andrés Bello, Santiago, Chile
[c] Advanced Mining Technology Center, Avda. Tupper 2007, Universidad de Chile, Santiago, Chile

ARTICLE INFO

Article history:
Received 25 August 2015
Received in revised form 14 October 2015
Accepted 8 November 2015
Available online 10 December 2015

Keywords:
Flat-slab segment
Doubly vergent fault system
Inverted fault
Mesozoic extensional fault systems

ABSTRACT

The Andean orogenic belt, located in the Central Andes "Pampean flat-slab" segment in northern Chile (27–29°S), is composed of two major tectonic regions: the Coastal Cordillera and the Frontal Cordillera. To understand their internal tectonic styles, history of growth and the shortening absorbed by the upper crustal structure of this segment, we combined regional geological mapping data, new ages obtained from radiometric U–Pb dating, and a semibalanced and restored cross-section 225.18 km in length. The results as shown in the previous Mesozoic extensional fault systems, established in northern Chile by the Gondwana breakup, have played a fundamental role in the orogenic buildup. The central structure is characterized by an asymmetric basin (Upper Cretaceous–Paleocene) confined by a doubly vergent fault system composed of inverted faults related to the edges of the Mesozoic Chañarcillo and Lautaro Basins. The U–Pb geochronological data obtained from synorogenic volcano-sedimentary deposits and the angular unconformities recorded between the Cenozoic geological units have revealed that the compressive deformation in this segment started at around ~80 Ma by tectonic inversion in the eastern Coastal Cordillera and western Frontal Cordillera, however, the presence of Paleocene and Miocene synorogenic successions at the footwall of the basement reverse faults of the Frontal Cordillera suggests a migration of Andean deformation from the west to the east during the Paleocene–Miocene by propagation of ramps involving inherited basement highs. The pre-compression restoration makes it possible to estimate 40.94 km of minimum shortening, concentrated by inversion anticlines and fault-controlled basement highs across the Frontal Cordillera.

1. Introduction

The Central Andes (Fig. 1) is an orogenic belt produced by crustal shortening, thickening, and magmatism related to the subduction of the oceanic Nazca Plate beneath continental South America (Ramos, 2009). The segmentation of the Nazca Plate beneath the Central Andes (steep subduction segment (15–24°S) and the flat-slab or "Pampean" subduction segment (28–33°S); Fig. 1) (Baraganzi and Isacks, 1976; Bevis and Isacks, 1984; Cahill and Isacks, 1992; Isacks, 1988; Jordan et al., 1983) has induced notable differences in the along-strike tectonic style, as well as the presence or absence of active volcanism in this orogenic belt. The tectonic styles and the geological processes related to the flat-slab subduction segment in the Central Andes have been better recorded on the eastern side of this orogenic belt (Fig. 1), as a result of the combination of a more advanced structural stage of evolution of this segment and an outstanding level of exposure due to the aridity of the mountains at these latitudes. A significant amount of the structural knowledge of this Andean segment has been derived from the large Sierras Pampeanas (SP in Fig. 1) and the petroliferous basins located in northwestern Argentina, between 24° and 33°S (e.g., the Santa Bárbara System, the Cordillera Oriental, the Tucumán Basin, the El Metán Basin, and others). These basins were initiated as NE and NW back-arc rift systems during the Cretaceous crustal stretching of the western South America, which occurred coeval with the opening of the South Atlantic Ocean and finally were deformed by the Andean compression during Cenozoic times (Grier et al., 1991; Kley and Monaldi, 1998; Ramos, 2009; Iaffa et al., 2011, among others).

Previous studies of this segment have taken advantage of two-dimensional (2-D) and three-dimensional (3-D) seismic information and deep oil well data, which have made it possible to identify special structural features, such as thick-skinned thrust systems, characterized by steeper faults in the crystalline basement, basement-involved compressive folds, reactivated faults, and shortening estimates of no more than 150 km (Carrapa et al., 2011; Coutand et al., 2001; DeCelles et al.,

* Corresponding author at: Departamento de Geología, Facultad de Ciencias Físicas y Matemáticas, Universidad de Chile, Plaza Ercilla 803, Santiago, Chile.
E-mail addresses: martinezfjh@hotmail.com (F. Martínez), cearriag@ing.uchile.cl (C. Arriagada), geodeckart@gmail.com (M. Peña), kdeckart@ing.uchile.cl (K. Deckart), rcharrie@ing.uchile.cl (R. Charrier).

http://dx.doi.org/10.1016/j.tecto.2015.11.019
0040-1951/

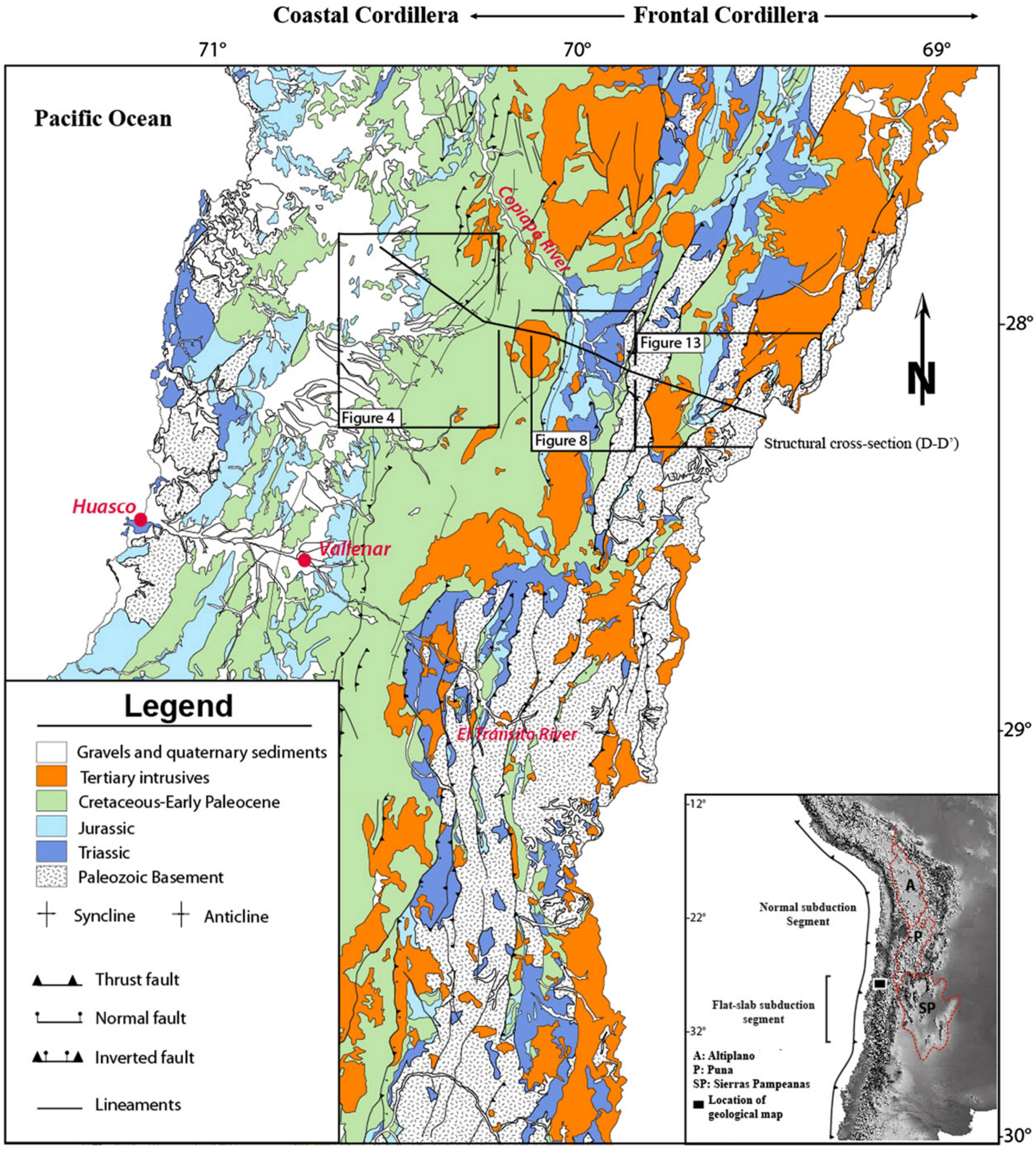

Fig. 1. General geological map of northern Chile between ~27°S and 30°S, showing the distribution of the main geological units and tectonic features.

2011; Iaffa et al., 2011; Jordan et al., 1983; Kley and Monaldi, 1998; Kley et al., 1999; Ramos et al., 2002). On the other hand, the timing of the onset of Andean deformation in this segment has been traditionally believed to occur as a major compressive pulse during the Neogene time on both, the Chilean and Argentinean sides (Jordan et al., 1983; Moscoso and Mpodozis, 1988; Ramos et al., 2002), however, new studies carried out on the western side have reported the oldest ages for the Andean deformation (Late Cretaceous–Paleocene) and a more complex tectonic evolution (Arriagada et al., 2006; Martínez et al., 2015; Peña et al., 2013). This situation has opened a new debate on the chronology of deformation in the region.

In contrast to the eastern side, the tectonic styles of the western side of the Central Andes in northern Chile (Fig. 1) have received little attention and have been poorly understood, so this represents a gap in the complete understanding of the anatomy of the orogenic belt at this latitude. This gap can be attributed to the lack of balanced cross-sections, the lack of geophysical interpretation of the subsurface, and the large metamorphic and igneous regions that make structural correlations difficult. Only a few structural studies of this region have been conducted (Amilibia et al., 2008; Arriagada et al., 2006, 2008; Martínez et al., 2012, 2013, 2015). These studies, which relied predominantly on surface data, have provided some background on the structural styles and ages of deformation recorded in some specific basins of this region.

Our objective in this research was to combine the results of recent studies (Martínez et al., 2012, 2013 and 2015) with new chronological data to produce a complete tectonic framework of the orogenic belt in northern Chile, from the Coastal Cordillera to the Frontal Cordillera (Figs. 1 and 2). We combined these data with tectonic models proposed for the Sierras Pampeanas in Argentina to obtain a regional

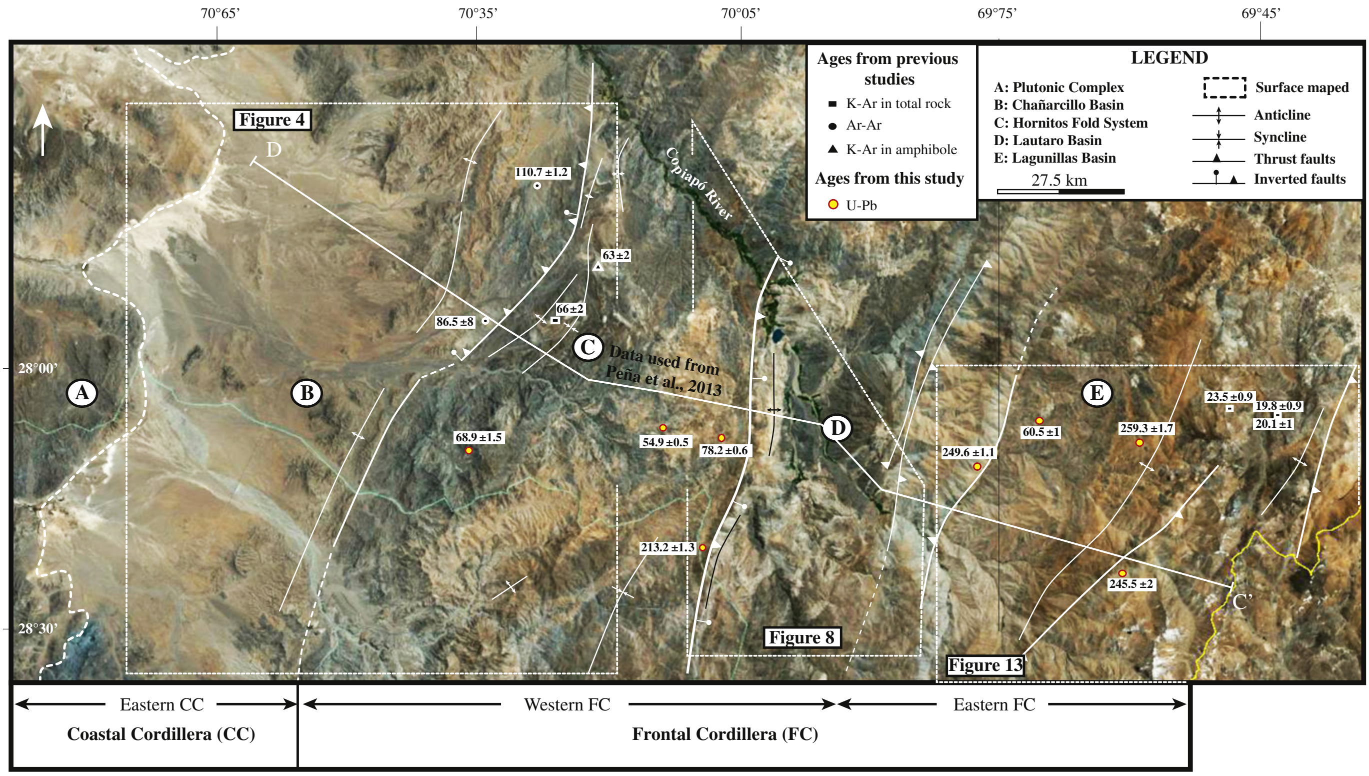

Fig. 2. Satellite image of the Andean segment analyzed in northern Chile (27–28°S), showing the tectonic domain distribution and the location of the semibalanced cross-section (D–D′) used in this study.

representation of the current structure of the Central Andes along the flat-slab segment. This paper describes the integration of regional mapping data with a regional semibalanced cross-section based on field observations. In addition, previously published radiometric ages from basement blocks and eight new radiometric ages from Mesozoic to Cenozoic deposits were used to obtain to complete a better chronology of the compressional deformation of the orogenic belt in this region.

2. Geological setting

2.1. Coastal Cordillera

The basement of the Chilean Coastal Cordillera between 27° and 29°S consists of Devonian to Carboniferous metasedimentary rocks intruded by plutonic complexes, with K/Ar, Ar/Ar and U/Pb ages of 190–180, 150–140, 120–130, and 110–90 Ma (Bahlburg and Breitkreuz, 1993; Bell, 1984; Dallmeyer et al., 1996; Grocott and Taylor, 2002; Naranjo and Puig, 1984; Scheubert and Reutter, 1992) (Fig. 2). These plutonic complexes are covered by volcanic and sedimentary deposits related to the Early Jurassic and Early Cretaceous magmatic arc and extensional back-arc basins (Mpodozis and Ramos, 2008; Oliveros et al., 2006). Different to those Cretaceous extensional systems developed in northwest Argentina and related to purely crustal extension, the extensional system of the Chilean side is mainly associated with a roll-back subduction geodynamic context established in western South America during the Gondwana breakup (Aguirre-Urreta, 1993; Franzese and Spalletti, 2001; Grocott and Taylor, 2002; Mpodozis and Kay, 1990; Mpodozis and Ramos, 1990, 2008; Pindell and Dewey, 1982; Ramos, 2009).

The Jurassic successions include andesitic flows, basaltic andesitic and volcanic breccias, and other volcanic successions that are part of the La Negra and Punta del Cobre Formations (Fig. 3) (Lara and Godoy, 1998; Marschik and Fontboté, 2001; Oliveros et al., 2006; Taylor et al., 2007). To the east of the Coastal Cordillera, the stratigraphic successions are defined as the Chañarcillo Basin infill (Fig. 4). In this basin, the Jurassic Punta del Cobre Formation is partially overlapped by approximately 4000 m of lower Cretaceous calcareous and siliciclastic syn-rift deposits that define the Chañarcillo Group (Figs. 3 and 4) (Arévalo, 1999; Mourgues, 2004; Price et al., 2008; Segerstrom, 1960; Segerstrom and Parker, 1959; Segerstrom and Ruiz, 1962). The Chañarcillo Group is unconformably covered by ~4000 m of Late Cretaceous (110.7 ± 1.7 and 99.7 ± 1.6 Ma U–Pb) (Macksaev et al., 2009) conglomeratic and volcanoclastic successions defined as the Cerrillos Formation (Arévalo, 1994, 2005a, 2005b; Jensen and Vicente, 1976; Marschik and Fontboté, 2001; Segerstrom and Ruiz, 1962). Based on its angular position over the Chañarcillo Group and the absence of: normal faults, internal progressive unconformities and drastic changes of thickness, the Cerrillos Formation has been attributed as to be the post-rift deposits of the Chañarcillo Basin (Martínez et al., 2013; Fig. 3).

The Cerrillos Formation is unconformably overlapped by nearly 2000 m of Upper Cretaceous–Paleocene deposits corresponding to the Hornitos Formation (Figs. 3 and 4) (Arévalo, 1994, 2005b; Arévalo and Welkner, 2008; Peña et al., 2013; Segerstrom, 1960). This succession is composed of intercalations of red sandstones, volcanic breccias, conglomerates, ignimbrites, and different volcanic flows that are intruded by different Paleocene plutonic complexes (Figs. 3 and 4). This formation has been interpreted as consisting of synorogenic deposits, and its accumulation was associated with the eastward-displaced magmatic arc (at approximately 85 Ma), according to Mpodozis and Ramos (1990) and Cornejo et al. (1993), and with volcano-sedimentary accumulations during the tectonic inversion of the Chañarcillo Basin (Martínez et al., 2013; Peña et al., 2013). Finally, Middle Miocene continental unconsolidated sediments (Atacama Gravels; Fig. 3) composed of horizontal packages of sands and gravels (Mortimer, 1973; Willis, 1929) unconformably overlie the folded and faulted Cretaceous and Paleocene deposits in this region and close the stratigraphic record (Fig. 4).

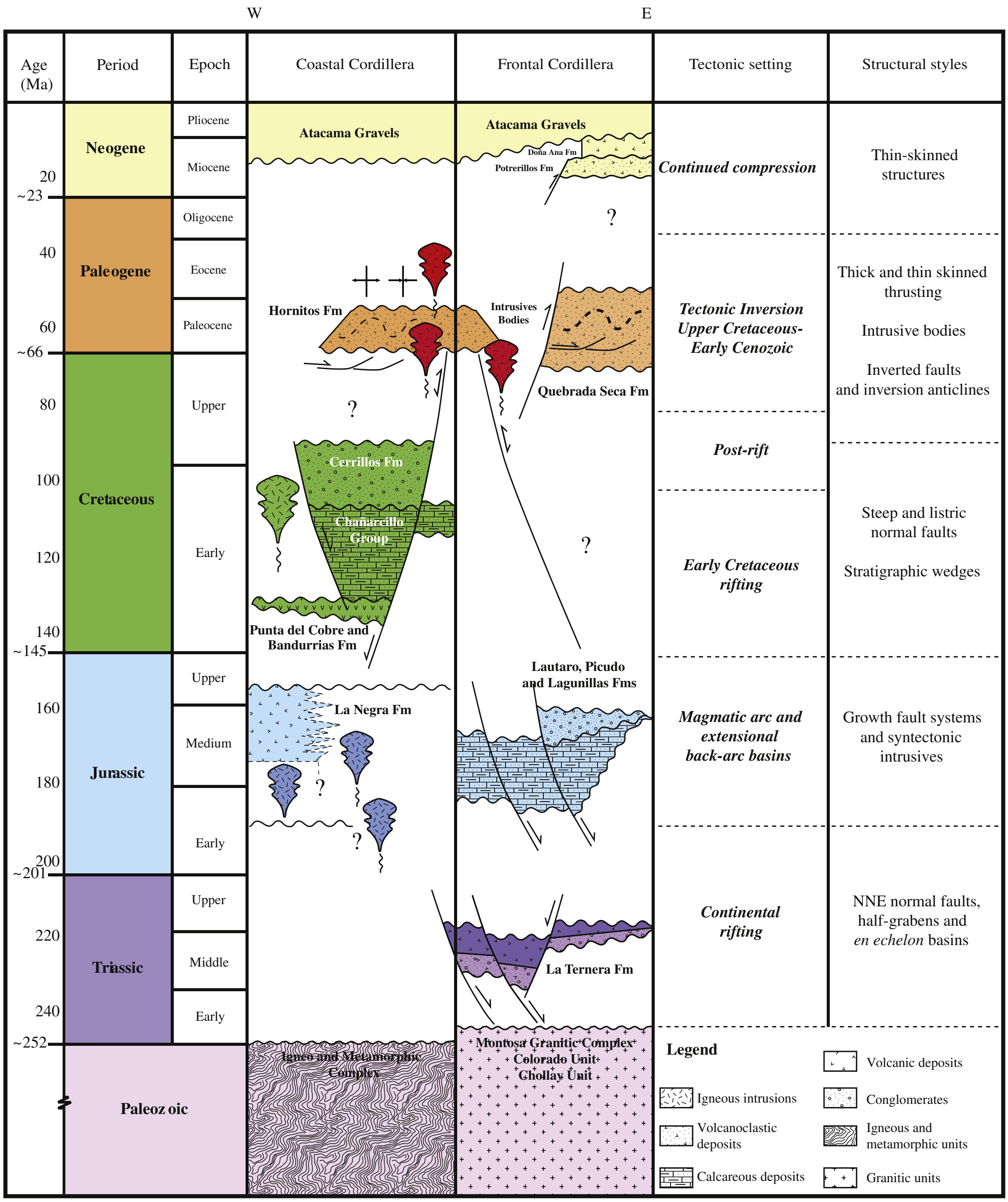

Fig. 3. Chronostratigraphic chart (after ICS, 2012) showing the sequences for the morphotectonic units and the different associated tectonic stages.

2.2. Frontal Cordillera

The Chilean Frontal Cordillera is composed mainly of late Paleozoic granitic basement blocks, exposed along a NNE-vergent E–W thrust system (Fig. 2) (Godoy and Davidson, 1976). These granitic rocks are mainly granodiorites, granites, and monzogranites that have K/Ar ages ranging from 263 to 228 Ma (Jensen, 1976; Moscoso et al., 2010; Mpodozis and Kay, 1990). Traditionally, they have been defined as the Montosa Granitic Complex or the Montosa Unit, the Las Juntas Pluton, and the Colorado and Chollay units (Farrar et al., 1970; Iriarte et al., 1999; Jensen, 1976; Moscoso et al., 2010; Mpodozis and Kay, 1990; Soffia, 1989; Zentilli, 1974).

The Frontal Cordillera is flanked on both the east and west sides by thick continental and marine syn-rift successions that rest unconformably on the Paleozoic basement (Figs. 8 and 13) (Charrier et al., 2007; Jensen, 1976; Martínez et al., 2012; Reutter, 1974). These syn-rift successions correspond to the Jurassic extensional Lautaro (western) and the Lagunillas (eastern) Basins (Charrier et al., 2007; Jensen, 1976; Martínez et al., 2012; Oliveros et al., 2013; Reutter, 1974). They are overlapped unconformably by younger Cenozoic volcano-sedimentary deposits, which have been interpreted as Andean synorogenic deposits locally intruded by Paleocene and Eocene plutons (Jensen, 1976; Moscoso and Mpodozis, 1988; Segerstrom, 1960) (Figs. 8 and 13).

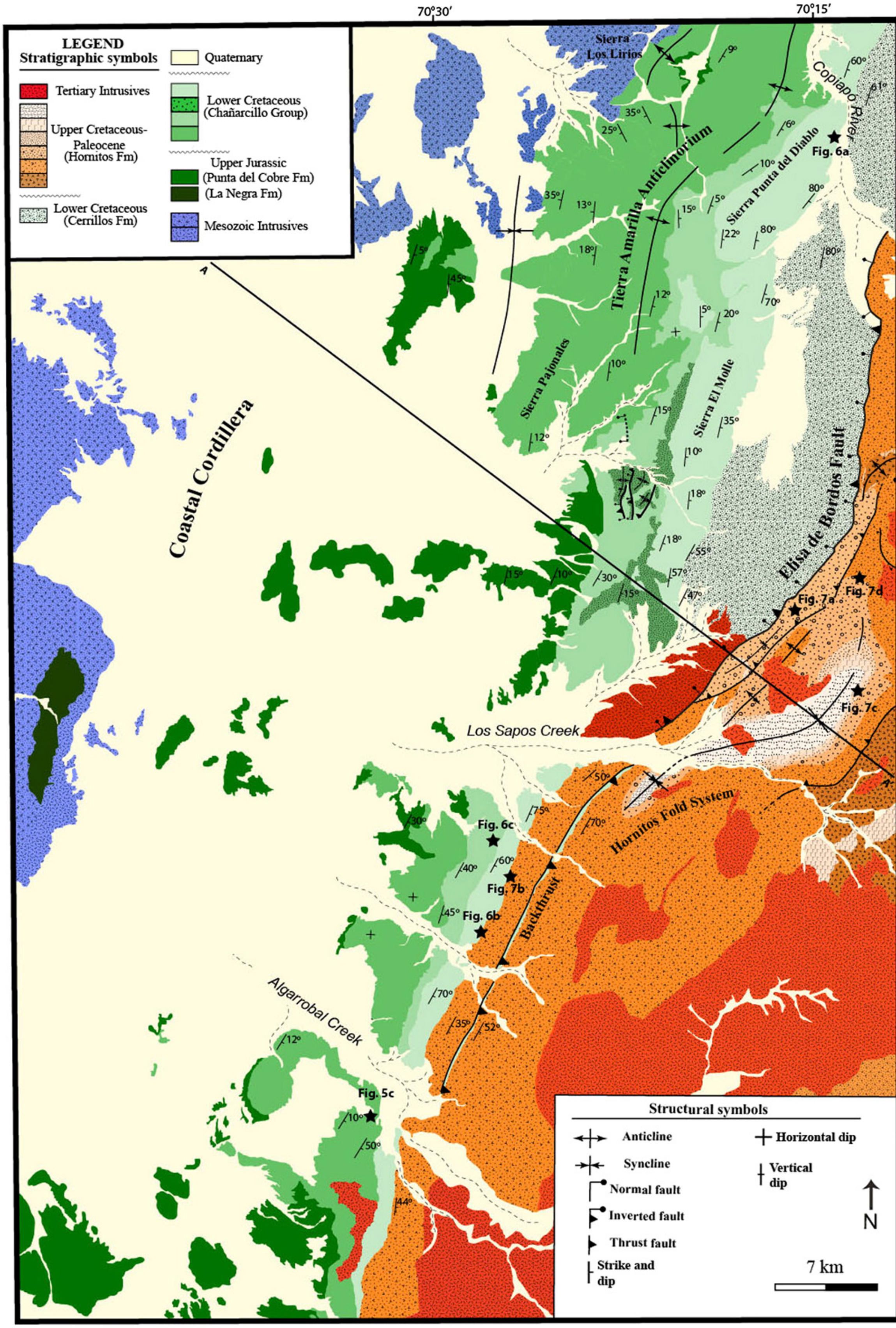

Fig. 4. Geological map of the Chañarcillo Basin along the eastern Coastal Cordillera. The location is outlined in Figs. 1 and 2.

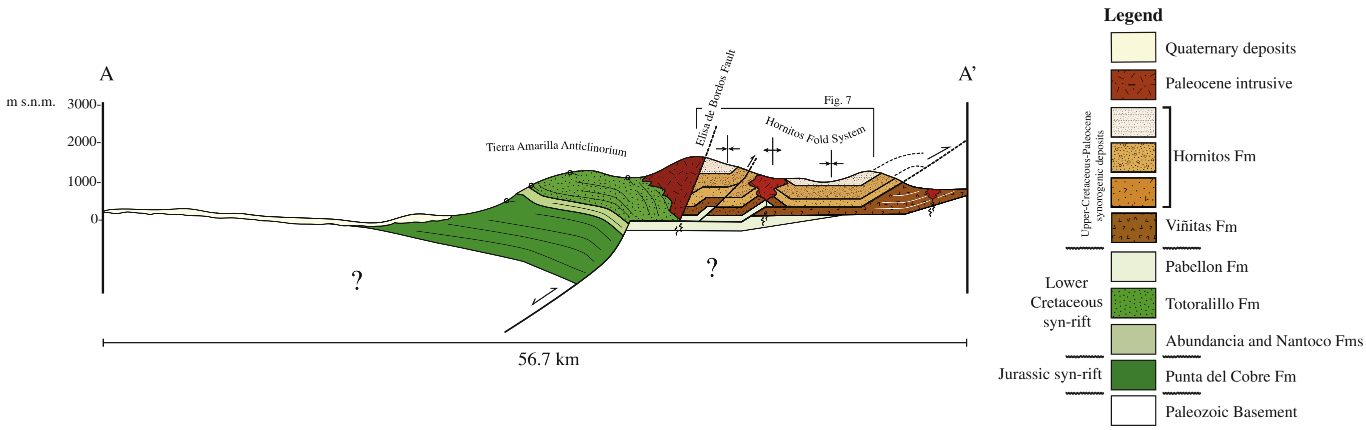

Fig. 5. Geological cross-section of the Chañarcillo Basin and the eastern flank of the Hornitos Fold System. See location in Fig. 4.

The best stratigraphic relationships can be observed along the Copiapó River section in the western Frontal Cordillera (Fig. 8). In this sector, outcrops show an excellent record of the Mesozoic infill of the Lautaro Basin, which is represented by a Late Triassic volcano-sedimentary syn-rift succession, approximately 2100 m thick, that is defined by the La Ternera Formation and includes intercalations of conglomerates, sandstones, lavas, basaltic andesites, and volcanic breccias (Figs. 3 and 8) (Charrier, 1979; Jensen, 1976; Martínez et al., 2012; Mpodozis and Cornejo, 1997; Reutter, 1974; Segerstrom, 1960; Sepúlveda and Naranjo, 1982; Suárez and Bell, 1992) and nearly 3000 m of Early Jurassic (Sinemurian–Bajocian) marine (limestones) and continental syn-rift successions (sandstones and shales) of the Lautaro and Picudo Formations (Figs. 3 and 8) (Arévalo, 1994, 2005a; Iriarte et al., 1999; Jensen, 1976; Jensen and Vicente, 1976; Martínez et al., 2012; Segerstrom, 1960; Soffia, 1989).

Other outcrops located to the east of the Frontal Cordillera show the complete Lagunillas Basin infill (Fig. 13). In this sector, the older deposits consist of the syn-rift volcano-sedimentary successions assigned to the Upper Triassic La Ternera Formation, which are covered by 3000-m-thick deposits consisting of conglomerates, sandstones, and calcareous intercalations that correspond to the Jurassic syn-rift successions of the Lautaro and Lagunillas Formations. The Mesozoic deposits are unconformably covered by nearly 1000 m of Paleocene volcanic and sedimentary deposits (conglomerates, red sandstones, andesites,

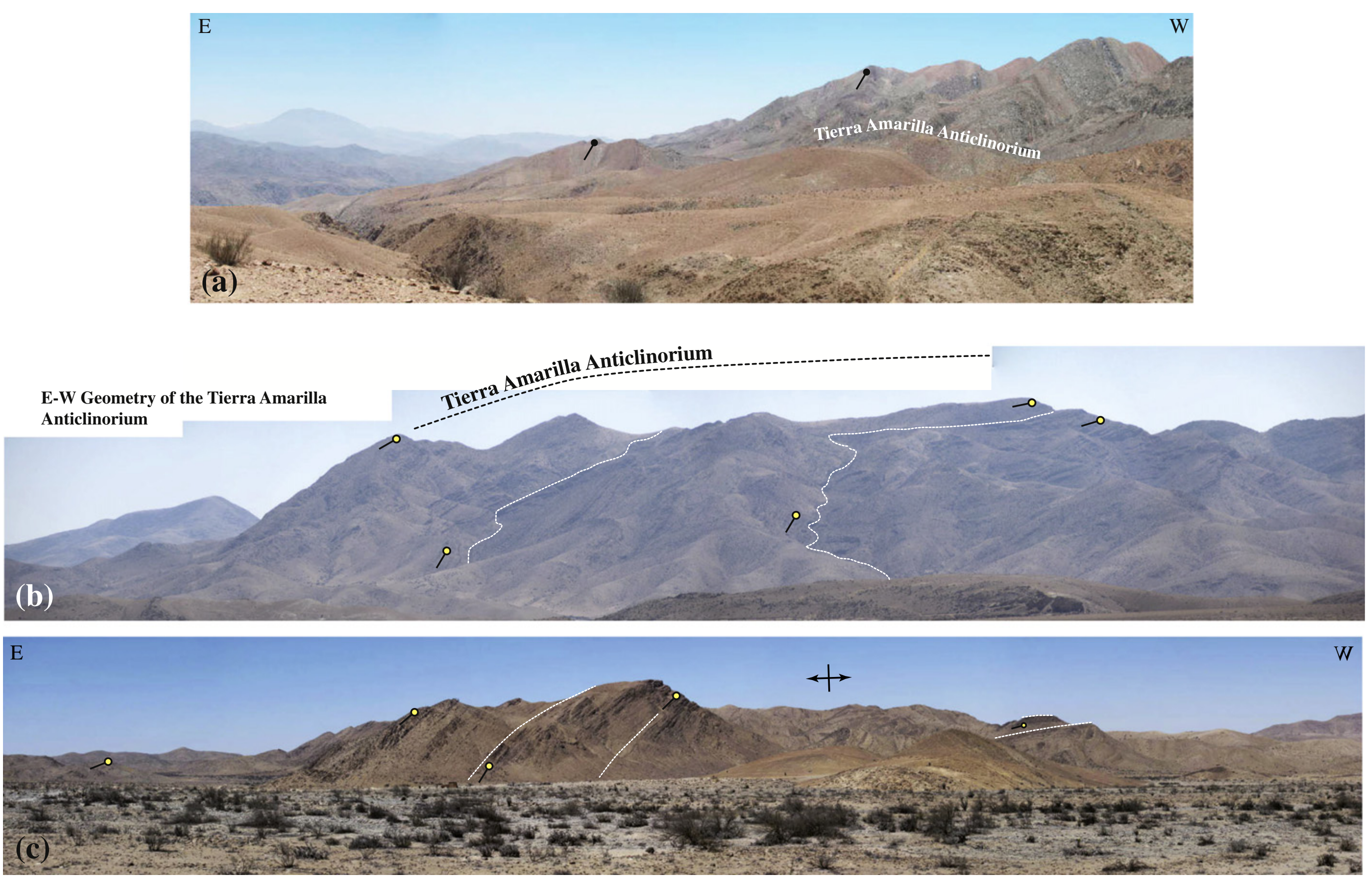

Fig. 6. Panoramic views of the main structure of the Chañarcillo Basin: a) position of the Tierra Amarilla Anticlinorium frontal limb at the Sierra Punta del Diablo location; b and c) geometry associated with an eastward-vergent asymmetric anticline (Tierra Amarilla Anticlinorium) observed along the Los Sapos Creek and the Algarrobal Creek, respectively. See location in Fig. 4.

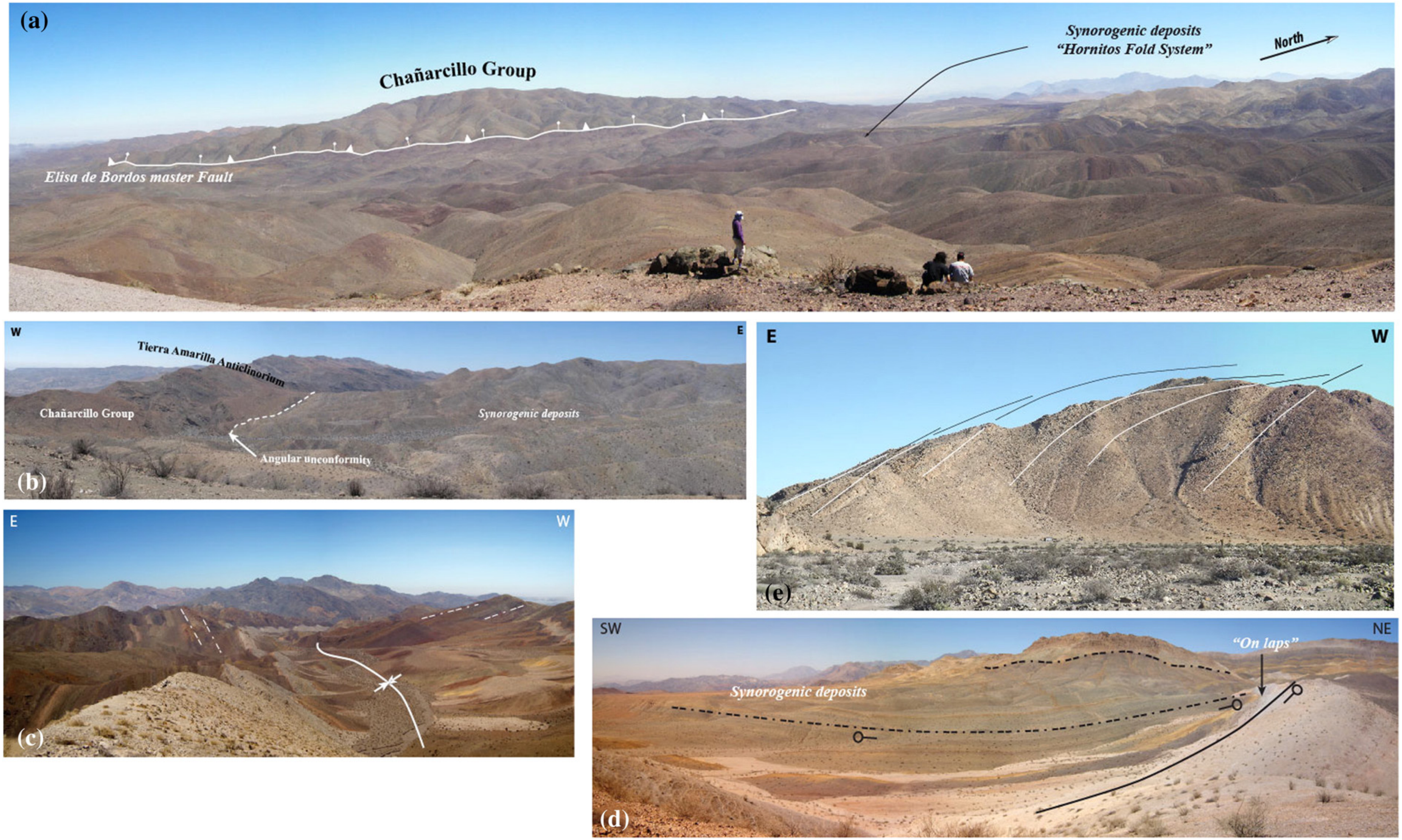

Fig. 7. a) Oblique aspect of the Elisa de Bordos Master Fault and the Early Cretaceous deposits thrust over the Paleocene synorogenic successions (Hornitos Formation); b) detail of the angular unconformity between the Chañarcillo Group and the Upper Cretaceous–Paleocene synorogenic deposits (Hornitos Formation); c) folding style recognized within the Hornitos Fold System; d) onlaps and progressive unconformities observed on the synclines of the Hornitos Fold System; e) detail of the wedge-shaped strata in the frontal limb of the Tierra Amarilla Anticlinorium. Note the progressive unconformities on the top of the strata. See location in Fig. 4.

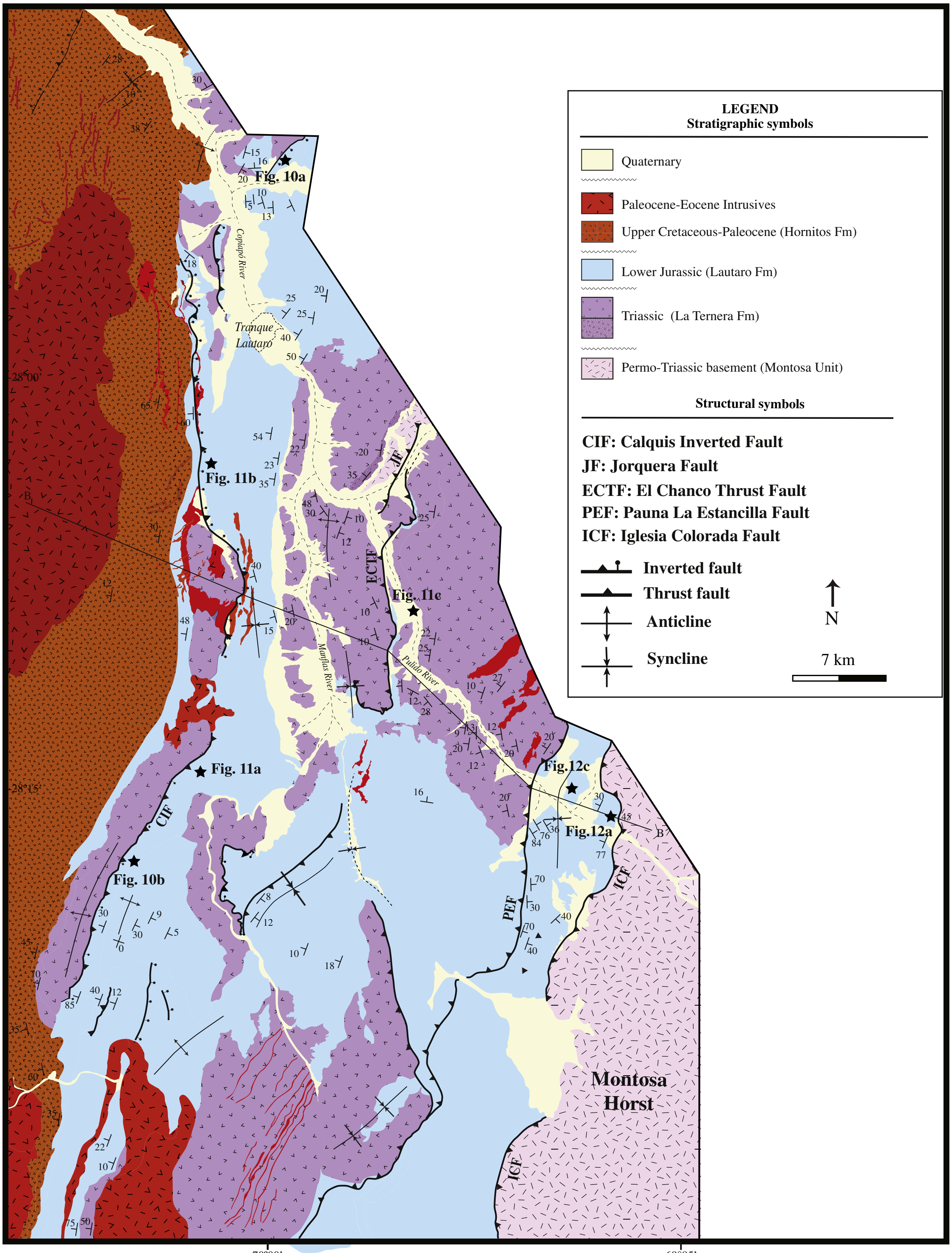

Fig. 8. Geological map of the Lautaro Basin along the western Chilean Frontal Cordillera. The location is outlined in Figs. 1 and 2.

and volcanic breccias) that correspond to the synorogenic Quebrada Seca Formation (Jensen, 1976; Moscoso et al., 2010; Soffia, 1989) (Figs. 3 and 13). The Quebrada Seca Formation is unconformably overlain by approximately 200 m of tilted Lower Miocene lacustrine conglomerates and sandstones, defined as the Potrerillos Formation (Jensen, 1976), as well as volcanic successions consisting of rhyolitic ignimbrite tuffs, lavas, dacitic flows, volcanic agglomerates, and breccias of the Doña Ana Formation (Martin et al., 1997; Thiele, 1964). Finally,

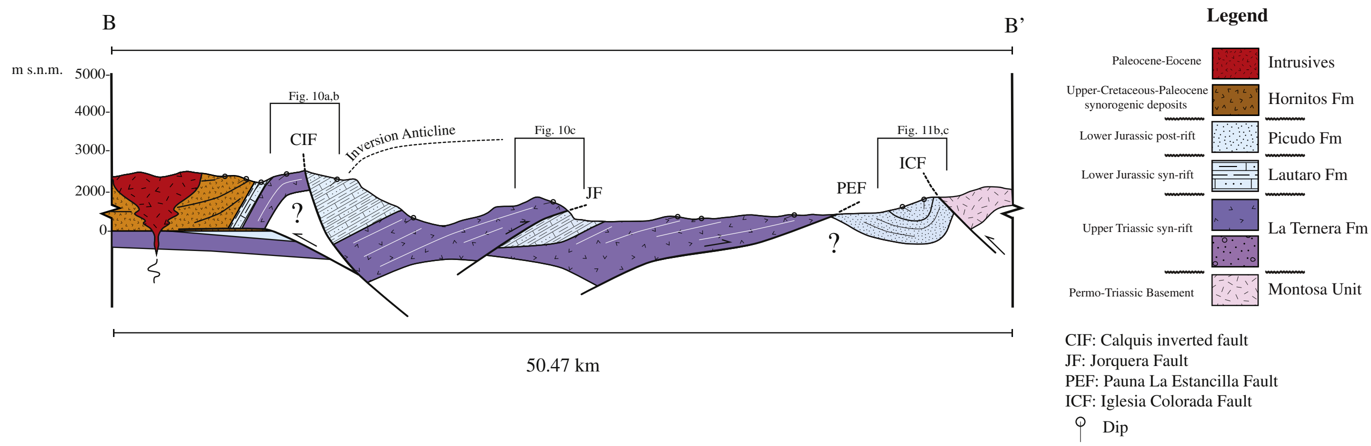

Fig. 9. Geological cross-section of the Lautaro Basin and the western flank of the Hornitos Fold System. See location in Fig. 8.

the stratigraphic record culminates with the Middle Miocene unconsolidated sediments of the Atacama Gravels described previously (Mortimer, 1973; Willis, 1929) (Figs. 3 and 13).

3. Methodology

3.1. Semibalanced cross-section

Several balanced cross-sections, supported by seismic, field, and oil well data, have permitted interpretations of the tectonic style of the thrust systems distributed along the Sierras Pampeanas of northwestern Argentina on the eastern side of the Andean flat-slab segment (Allmendinger et al., 1990; Jordan and Allmendinger, 1986; Kley et al., 1999; Ramos et al., 2002; Zapata and Allmendinger, 1996). However, on the Chilean side, there are few regional cross-sections that illustrate the tectonic style that dominates the western regions. We have created the first regional cross-section (D–D′) on the Chilean side, from the Coastal Cordillera to the Frontal Cordillera (225.18 km in length) (Figs. 1 and 2). We have also incorporated structural information from a cross-section through the Sierras Pampeanas (Ramos et al., 2002) to provide a more regional view of the Andean structure across the entire orogen.

We created the cross-section (D–D′) using the 2D MOVE software, integrating the geological information shown in Figs. 4, 8, and 13,

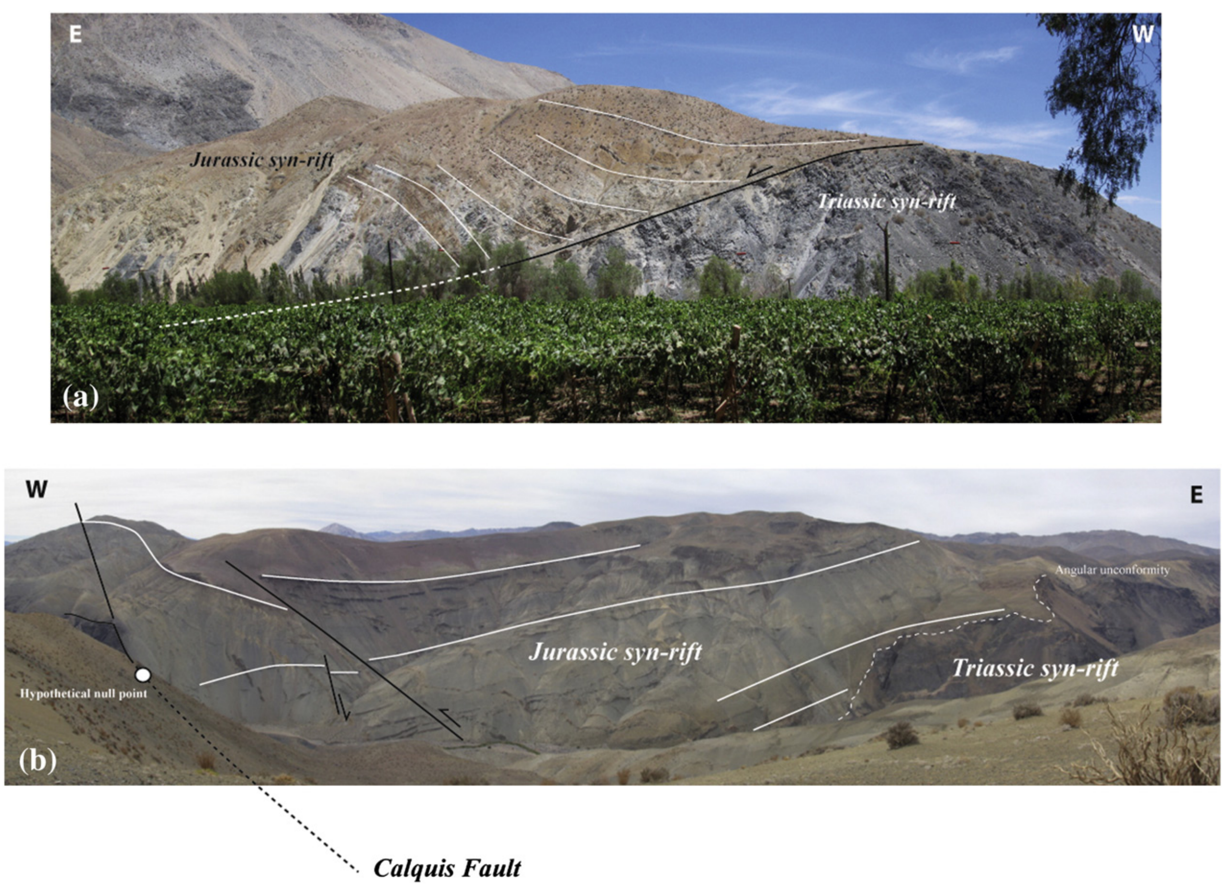

Fig. 10. a) Detail of the mesoscale synextensional normal fault and growth strata in the Lautaro Formation; b) inversion anticline with "harpoon geometry" illustrating the partial reactivation of the Calquis Fault. See locations in Fig. 8.

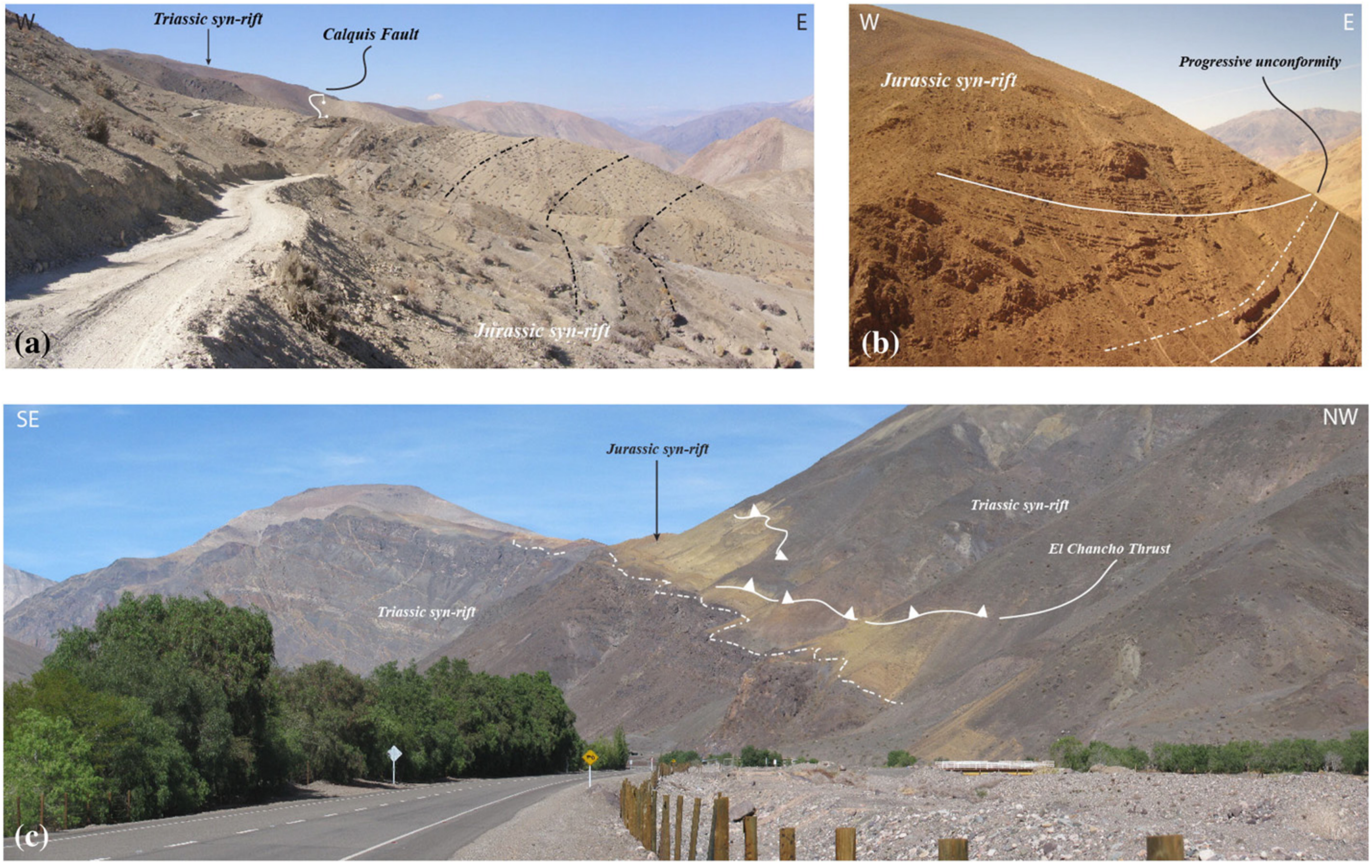

Fig. 11. a) Buttressing of the Jurassic syn-rift series against the Master Calquis Fault along the western Lautaro Basin; b) extensional progressive unconformities identified within the Lautaro Formation; c) panoramic view of the southwestward-vergent El Chancho Thrust along the Copiapó River in the Lautaro Basin. See location in Fig. 8.

reported in previous studies (Martínez et al., 2012, 2013, 2015). We also filled in the gap between the geological maps in Figs. 4 and 8 using the geological information reported by Peña et al. (2013). The cross-section was first designed by hand and by honoring stratigraphic thicknesses and dip attitudes. However, in some places where the surface geological information is insufficient, the ramp cutoff angles and some stratigraphic thickness were assumed. Given the assumptions made, we considered this a semibalanced cross-section, because this can be a critical issue for some experts. We then performed a step-by-step restoration to a final pre-shortening state. Line lengths were used to restore the thin-skinned faults and folds, and area preservation was used to restore the basement faults. Forward modeling was carried out to test the complete configuration of the interpreted structures. Based on trial and error, we used a hypothetical basal detachment positioned at 10 km depth, and finally, we attempted to reproduce and quantify the geometry and shortening observed at the surface. However, this could be deeper according to the intracrustal density discontinuities under the Sierras Pampeanas in Argentina interpreted by Alvarado and Ramos (2011).

3.2. U–Pb LA-ICPMS geochronology

Eight zircon samples were prepared and separated using standard preparation methods in the Geology Department of the University of Chile, using the Gemeni table, a Frantz magnetic separator, and heavy liquid procedures. Final grain selection was undertaken by hand, using a binocular microscope. The mineral samples were sent for analyses to the Laboratory of Isotopic Studies (LEI) of the Geoscience Center of the National Autonomous University of Mexico (UNAM).

The analytical work was undertaken using a Resonetics Resolution M50 193-nm laser Excimer connected to a Thermo Xii Series Quadrupole Mass Spectrometer, following analytical procedures and technical details described by Solari et al. (2010). The laser ablation diameter was fixed at 34 μm. Ages were calculated using Isoplot v. 3.7 (Ludwing, 2008). Intrusive ages were calculated using the algorithm of the TuffZirc program, and mean ages were calculated using Isoplot v. 3.7 (Ludwing, 2008). The results are summarized in tables in the Supplementary Data 1.

4. Tectonic styles

4.1. The Coastal Cordillera

Western section: In the study area, this section is characterized by an extensive exposure of outcrops of Lower Jurassic and Lower Cretaceous granitic rocks (Brown et al., 1993; Grocott and Taylor, 2002) (Fig. 2). Previous studies (Arévalo and Welkner, 2008; Dallmeyer et al., 1996; Grocott and Taylor, 2002; Taylor et al., 1998) have reported a structural style of NW- and NE-trending fault zones characterized by steep normal faults with a minor left-lateral strike slip component, identified by kinematic indicators (Grocott and Taylor, 2002). However, these fault systems are not clearly exposed in our study area.

Eastern section: At the eastern limit of the Coastal Cordillera, specifically in the Chañarcillo Basin (Figs. 2 and 4), the main structure is a large sinuous eastward-vergent anticline, called the Tierra Amarilla Anticlinorium by Segerstrom and Ruiz (1962). This fold extends along a NNE strike from the Copiapó River Valley to the Algarrobal Creek (Fig. 4). The fold has a long wavelength with an asymmetrical eastward-vergent geometry, characterized by an almost subhorizontal western back limb and an inclined frontal limb (45–80°E, Fig. 5), which is truncated by the Elisa de Bordos Master Fault toward the east (Figs. 4 and 5). This fold involves the syn-rift deposits of the

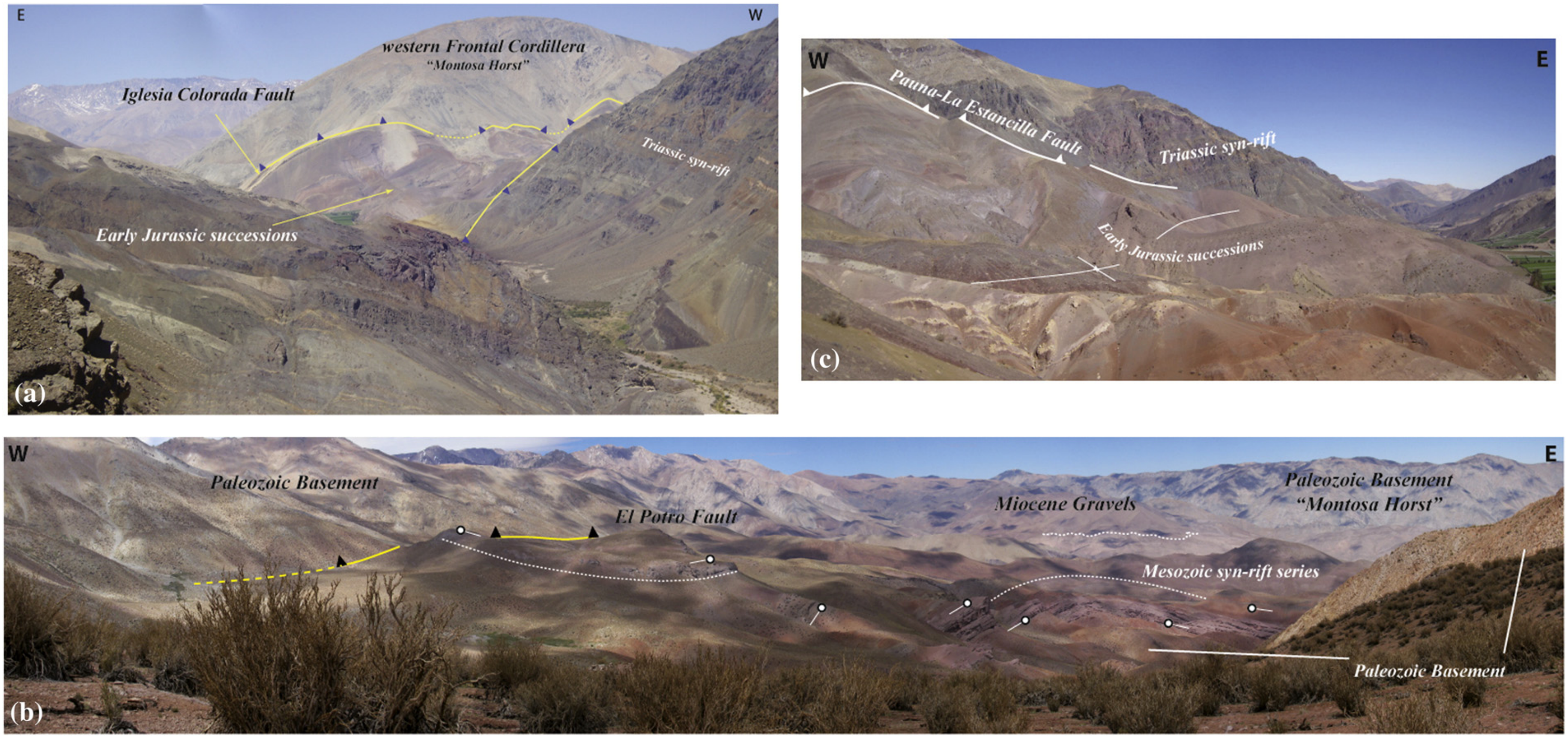

Fig. 12. a) Frontal view of the Iglesia Colorada Fault and the Montosa Horst in the western Frontal Cordillera. Observe the triangular zone between the Iglesia Colorada and the Pauna–La Estancilla Fault; b) panoramic view of the Colorado–El León Anticline toward the east of the Montosa Horst; c) footwall syncline associated with thrusting of the Pauna–La Estancilla Fault. See location in Figs. 8 and 13.

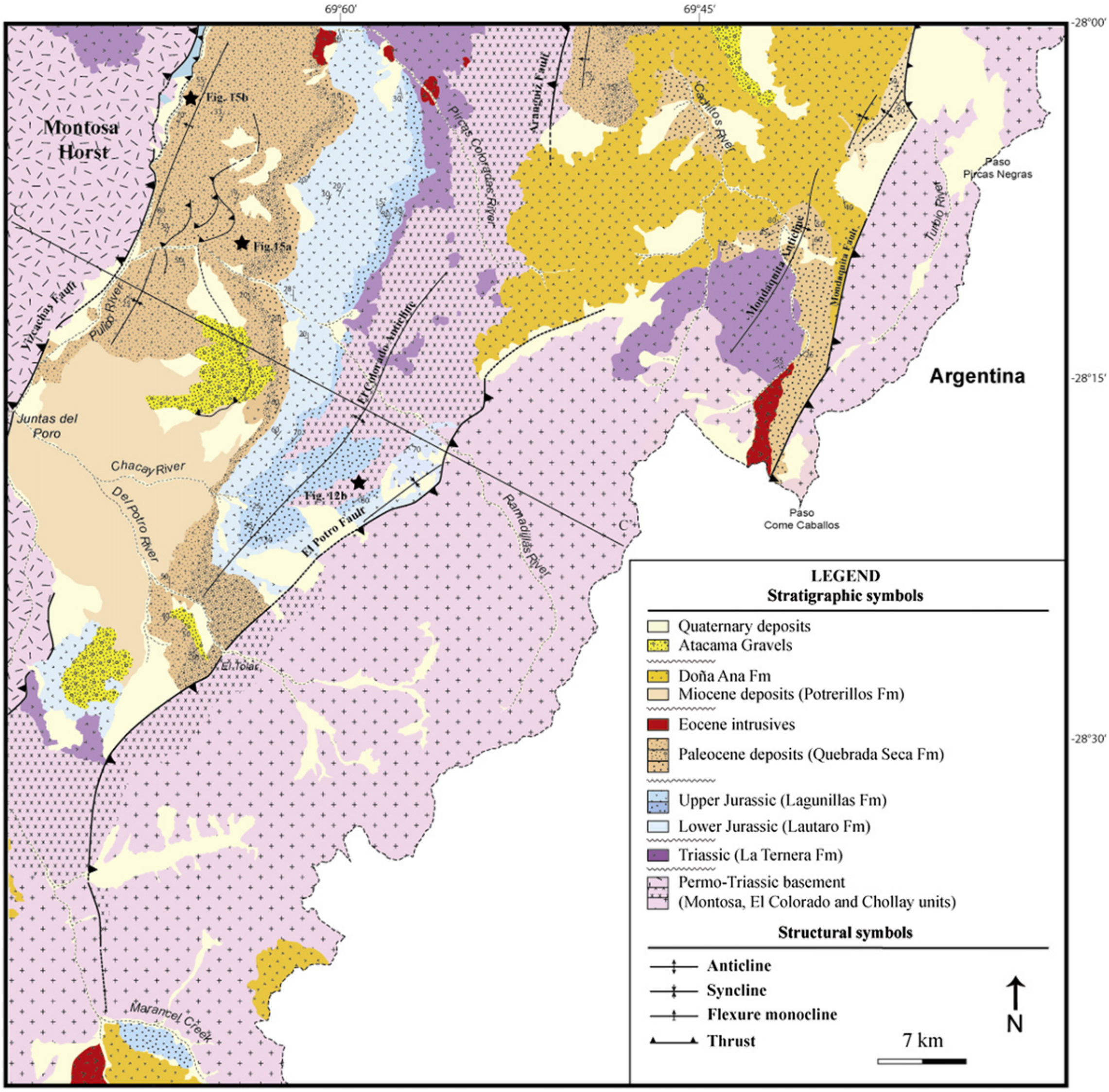

Fig. 13. Geological map of the Lagunillas Basin along the eastern Chilean Frontal Cordillera. The location is outlined in Fig. 1 and 2.

Cretaceous Chañarcillo Group and the Punta del Cobre Formation, as well as the post-rift volcano-sedimentary successions of the Cerrillos Formation. It is locally affected by Paleocene intrusive bodies in its frontal limb (Fig. 4). Along the anticline, large variations in the stratigraphic thickness of the Chañarcillo Group are noted between the frontal (>~2000 m) and back limbs (<1000 m). This situation defines a typical stratigraphic wedge that is thicker toward the Elisa de Bordos Fault (Fig. 6) (Martínez et al., 2013). Additionally, a series of synextensional features is preserved within the Chañarcillo Group, such as extensional growth strata and synsedimentary normal faults (Fig. 7e).

Based on this structural and stratigraphic relationship, the Tierra Amarilla Anticlinorium could be an inversion anticline (Yamada and McClay, 2003) linked to reactivation of the NNE high-angle Elisa de Bordos Master Fault (Martínez et al., 2013) (Fig. 5). Although the inversion anticline is the main structural style in the region, other minor westward-vergent thrusts or backthrusts have also been recognized as internally affecting the syn-rift deposits of the Cretaceous Chañarcillo Group. However, these are interpreted as accommodation faults that formed during the growth of the inversion anticline.

4.2. Frontal Cordillera

Western section: Through this section, two tectonic styles are recognized. The first is located immediately to the east of the Elisa de Bordos Fault (Figs. 4 and 5) and is represented by a narrow thin-skinned fold system (Hornitos Fold System), approximately 33 km in length (Martínez et al., 2013; Peña et al., 2010), involving mainly the Upper Cretaceous–Paleocene synorogenic deposits of the Hornitos Formation. The folds are characterized by NNE asymmetric synclines and minor anticlines related to thrust faults (Figs. 4, 5, and 7). Along this compressive system, most of the folds are located in the western sector (Fig. 5). In this sector, the asymmetric synclines are almost continuous, and the thrust faults run parallel to the beds (Figs. 4, 5, and 7). Furthermore, the synclines show well-developed growth strata, and several Paleocene and Eocene plutonic bodies are intruded along the fold axis (Fig. 7d) and generally obscure the structures. We have related this folding style with an eastward-vergent thrust that fed slip into the Hornitos folds with a flat-ramp geometry (Fig. 5).

The second tectonic style is represented by the structures of the Lautaro Basin (Figs. 8 and 9). The main structure consists of a long-wavelength, westward-vergent, asymmetric anticline approximately

20 km length that involves the Triassic and Jurassic syn-rift deposits (e.g., the La Ternera and Lautaro Formations). Along this fold, dramatic thickness changes and inherent extensional features (Figs. 10 and 11b) are observed in the Mesozoic syn-rift deposits, which form a typical wedge shape toward the western limit of the Lautaro Basin (Figs. 9 and 10). The anticline is confined to the hanging-wall block of the NNE-striking Calquis Fault (Figs. 8, 9, and 10), with an overturned frontal limb truncated to the west by the latter (Fig. 11a) and a semi-horizontal back limb. The NNE-striking Calquis Fault is a high-angle fault (70–80°) that marks the western limit of the Lautaro Basin (Figs. 8, 9, and 11). The footwall fault consists of a thin, westward-tilted, Upper Triassic syn-rift deposit of the La Ternera Formation, which is associated with a blind westward-vergent short-cut fault (Fig. 9).

The geometry of the deformation in the Lautaro Basin suggests that the deformation is the result of the partial tectonic inversion of the Lautaro Basin and especially of the buttressing of Mesozoic syn-rift deposits against the western limit of the basin or the Calquis Fault (Figs. 9 and 11a) (Martínez et al., 2012). According to this interpretation, the uplift and westward tilting of the footwall of the Calquis Fault can be associated with blind footwall short-cut structures affecting the syn-rift packages of the La Ternera Formation (Fig. 9). To the east of this sector, along the central section of the Lautaro Basin, a NE–SW eastward-vergent thrust system can be identified. This thrust system is composed of the Jorquera Fault, the El Chancho Thrust Fault, and the Pauna–La Estancilla Fault (Fig. 8). The Jorquera Fault is a thick-skinned structure that extends over 5 km and carries a thin sheet of Paleozoic rocks over the Triassic and Jurassic syn-rift deposits of the Lautaro and La Ternera Formations along the Jorquera River (Fig. 8). The thin-skinned El Chancho Thrust (Fig. 11c), exposed to the east of the Jorquera Fault, places the syn-rift deposits of the La Ternera Formation over the upper section of the Jurassic syn-rift deposits of the Lautaro Formation. The Pauna–La Estancilla Fault is a westward-dipping reverse fault that extends 35 km to the Copiapó River. Along the river (Fig. 12a and c), this fault is recognized as a thin-skinned structure with a hanging wall formed by the volcanoclastic successions of the La Ternera Formation and a footwall composed of the folded siliciclastic successions of the Lautaro Formation (Fig. 12a and c).

Eastern region: Large NNE-striking basement reverse faults (e.g., the Iglesia Colorada Fault, the Vizcachas Fault, the El Potro Fault, and the Mondaquita Fault; Figs. 8 and 13) affect large Permo-Triassic granitic blocks, as well as the Meso-Cenozoic deposits of the Lagunillas Basin. The structure consists of doubly vergent (E–W) basement reverse faults with moderate and high angles at the surface (50–70°) and basement-cored folds (e.g., the Montosa Horst and the Colorado–El León Anticline) (Figs. 8 and 13) (Godoy and Davidson, 1976; Jensen, 1976; Moscoso and Mpodozis, 1988; Reutter, 1974). The hanging walls of these faults reach up to 5500 masl, forming the most prominent topographic highs within the region. The Montosa Horst (Figs. 8 and 13) is limited on its western side by the westward-vergent Iglesia Colorada Fault (Fig. 12a) and on the eastern side by the eastward-vergent Vizcachas Fault (western edge of the Lagunillas Basin; Fig. 15), indicating a pop-up geometry. The footwall faults are characterized by a footwall syncline fold (Iglesia Colorada Fault; Fig. 12c) and by an overthrust anticline (Fig. 15) that involve both syn-rift Mesozoic (e.g., Lautaro Formation) and synorogenic Cenozoic deposits (Quebrada Seca Formation) (Figs. 8 and 13).

The eastward-vergent Colorado–El León Anticline is a basement-cored fold characterized by a low-angle back limb and a steeper frontal limb that involves syn-rift Mesozoic deposits (e.g., the La Ternera and Lagunillas Formations) (Figs. 12, 13, and 14) that can be related to an eastward-vergent blind thrust. To the east of the Colorado–El León Anticline, the Mondaquita–El Potro Fault System is exposed (Fig. 13). This fault is a westward-vergent basement thrust that represents the easternmost fault system in the study area. The Mondaquita–El Potro Fault

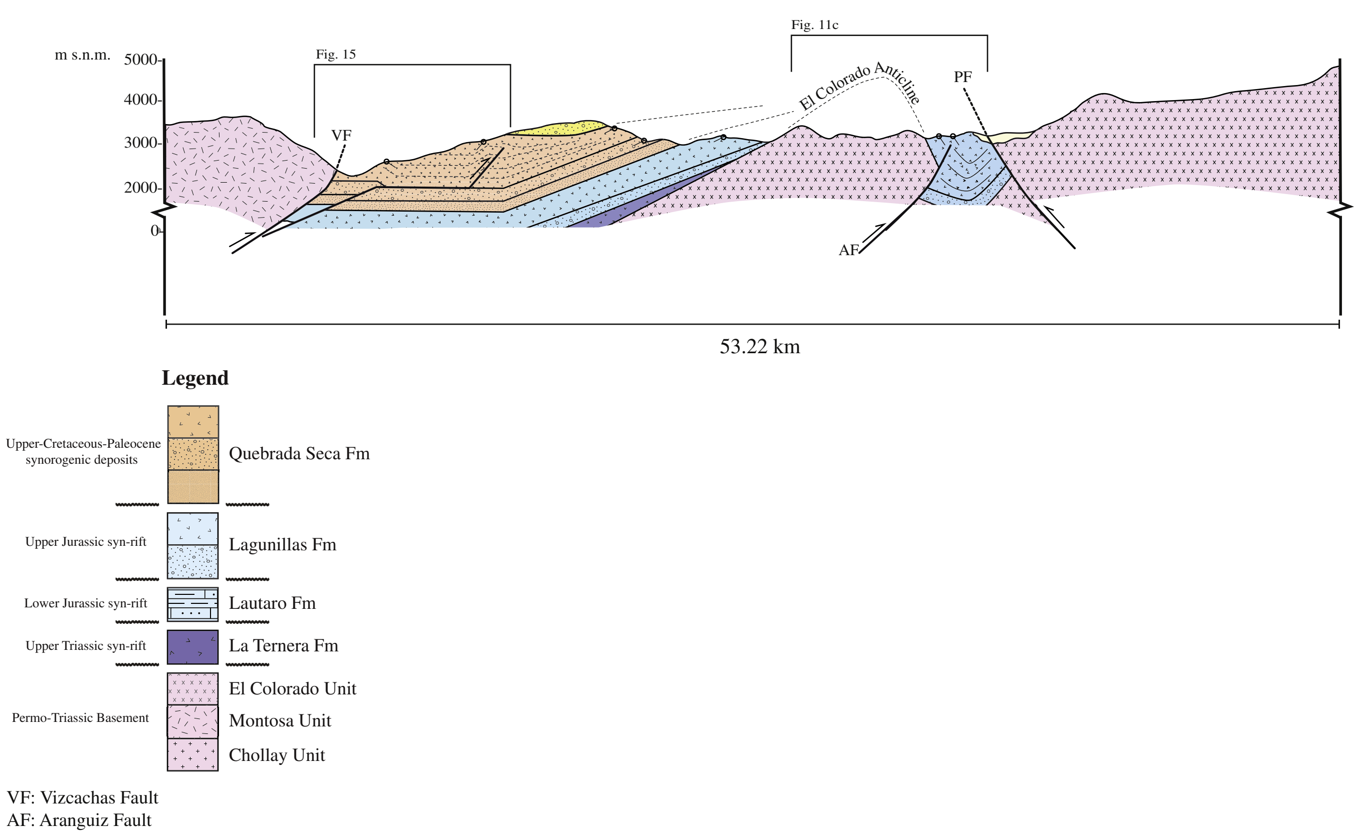

Fig. 14. Geological cross-section of the Lagunillas Basin and the eastern flank of the Chilean Frontal Cordillera. See location in Fig. 13.

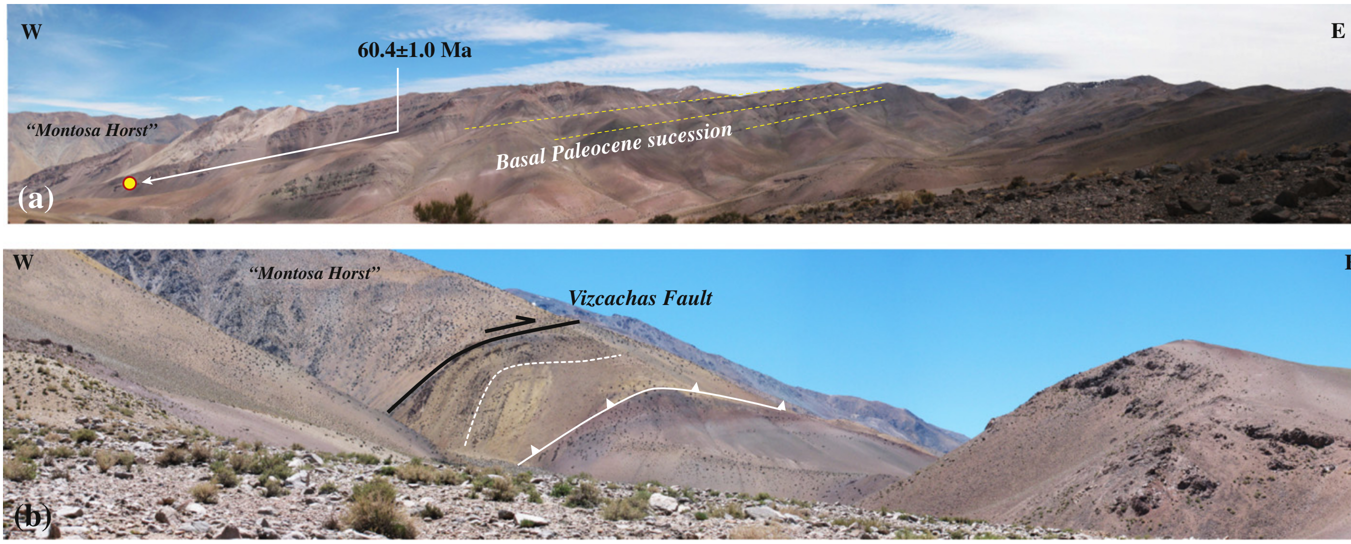

Fig. 15. a) Detail of the Paleocene packages overthrust by the eastward-vergent Vizcachas Fault recognized to the east of the Montosa Horst; b) aspect of the thick-skinned Vizcachas Fault and the Granitic Montosa Complex along the hanging-wall fault.

System carries a wide (~8 km) basement block over the Upper Jurassic syn-rift deposits of the Lagunillas Formation and truncates the frontal limb of the El Colorado–El León Anticline (Figs. 12 and 13).

5. Semibalanced cross-section and crustal shortening

In the cross-section D–D′, the structure of the Cretaceous Chañarcillo Basin is represented by a partially inverted half-graben, and the Tierra Amarilla Anticlinorium is produced from its partial reactivation (Fig. 16). The thin-skinned anticline and syncline of the Hornitos Fold System are reproduced and interpreted by a flat-ramp–flat-ramp geometry. We suggest that the motion of the hanging wall of this system could have transported the upper section of the Elisa de Bordos Fault toward the east (Fig. 16). We also suggest that the geometry of the Tierra Amarilla Anticlinorium was acquired initially from the partial reactivation of the Elisa de Bordos Fault but was then transported by the propagation of an eastward-vergent thin-skinned thrust system developed in the footwall of the Elisa de Bordos Fault. To model the structures of the Chañarcillo Basin and the Hornitos Fold System, we used two detachments: a basal detachment positioned at a depth of approximately 7 km, which can be projected within some ductile units below the western Coastal Cordillera, and an upper detachment located above the footwall of the Elisa de Bordos Fault (Fig. 16).

The western edge of the Lautaro Basin is interpreted as an eastward-vergent inverted half-graben with a basal detachment located at a depth of approximately 10 km. This western edge consists of a reactivated master fault (the Calquis Fault), which is accompanied by a subsidiary footwall short-cut fault that affects the eastern side of the Hornitos Fold System. Based on the restoration and forwarding of the structures recognized in this sector, we propose that both the thin- and thick-skinned faults exposed along the central section of the Lautaro Basin are reproduced mainly by eastward-vergent ramps, as illustrated in Fig. 16, and that these ramps are responsible for the uplift and overthrust of the Triassic syn-rift deposits. However, the El Chancho Thrust and Pauna–La Estancilla Fault constitute special situations because the drastic thickness change expressed by the Triassic syn-rift deposits in the footwall of both faults indicates that they could having propagated from the inherent normal faults (Fig. 16).

To the east of the Lautaro Basin, the configuration of the Chilean Frontal Cordillera is explained by the shortening of previous basement highs that were uplifted by large eastward-vergent ramps and other westward-vergent reverse faults (e.g., the Mondaquita Fault) (Fig. 16). Based on the positions of the syn-rift deposits along these structures, we suggest that the eastward-vergent thick-skinned system truncated the previous Mesozoic extensional systems developed in the region. Finally, we believe that the structure of this Andean segment can be explained by the tectonic inversion of the Mesozoic basins, followed by the eastward propagation of basement thrusts and folds (e.g., the Colorado–El León Anticline) (Fig. 16). The palinspastic restoration of deformation indicates an estimated 40.94 km of minimum shortening (Fig. 16), produced mostly by the eastward-vergent ramps across the Frontal Cordillera.

6. Ages of rocks and Andean deformation

Research carried out to the east of our study area, along the Pampean subduction segment (e.g., the Cordillera Oriental, the Santa Bárbara System, and the Sierras Pampeanas) indicates that Andean deformation took place mainly during the Neogene (Jordan et al., 1983; Allmendinger et al., 1997; Ramos et al., 2002; Carrera et al., 2006; Carrapa et al., 2011, among others). Other researchers have indicated that immediately to the north, at the southern edge of the Puna Plateau, the deformation started during the Late Cretaceous–Paleocene (Somoza, 1998; Cobbold et al., 2007; DeCelles et al., 2011).

In contrast, Andean deformation along the western slope of the Central Andes in northern Chile is believed to have begun during the Oligocene–Eocene (Jensen, 1976; Moscoso and Mpodozis, 1988; Soffia, 1989) but could have begun as early as 90–70 Ma in the Domeyko Cordillera and the Salar de Atacama Basin (Amilibia et al., 2008; Arriagada et al., 2006; Bascuñan et al., 2015; Charrier et al., 2013; Mpodozis et al., 2005; Steinman, 1929). Some studies have identified younger U–Pb ages in our study area and have suggested that compressional deformation occurred during the Late Cretaceous–Paleocene (60–65 Ma) (Maksaev et al., 2009; Martínez et al., 2013; Peña et al., 2013). Because of the wide range of ages proposed for the initiation of Andean deformation, we obtained new U–Pb ages from the synorogenic deposits to interpret the different deformation ages. We also obtained U–Pb ages from volcanic Triassic syn-rift deposits, as well as the basement rocks, to refine the chronology of the stratigraphic units exposed in the region (Supplementary Data 1 and Fig. 2). The chronological record obtained in this study was complemented using ages from previous studies (Arévalo, 2005b; Maksaev et al., 2009). All these data were employed to interpret the uplift and deformation age of the eastern Coastal Cordillera and the Frontal Cordillera.

The new U–Pb ages obtained from the plutonic complexes of the Frontal Cordillera (Supplementary Data 1 and Fig. 17) are 245.5 ±

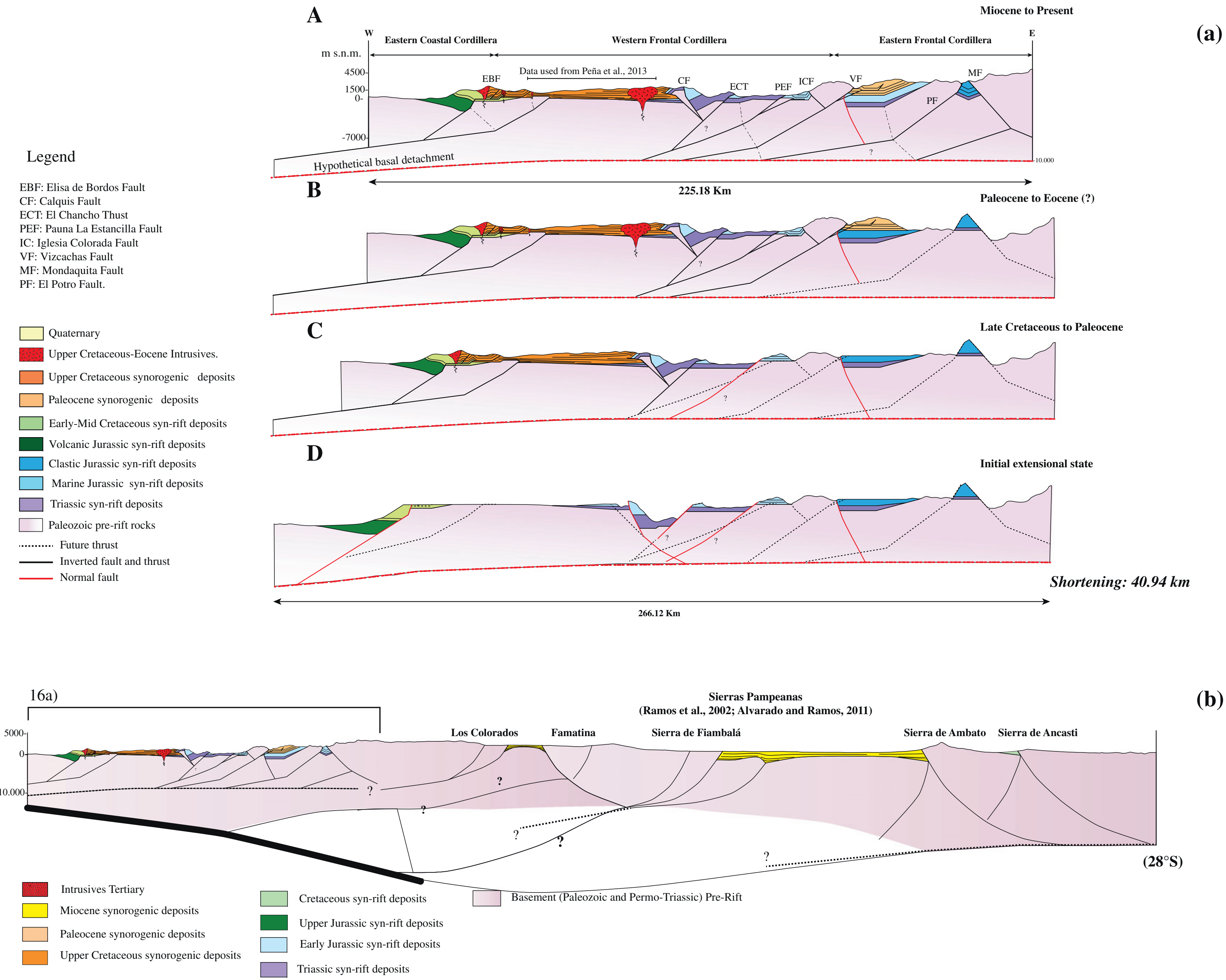

Fig. 16. a) Semibalanced cross-section (D–D′) and restoration to different depositional states of the flat-slab subduction segment in northern Chile (27–29°S). See location in Fig. 2; b) crustal cross-section of the Central Andes at 28°S latitude. This section integrates the semibalanced cross-section considered in this study and the crustal geological interpretations of Ramos et al. (2002) and Alvarado and Ramos (2011) for the neighboring Sierras Pampeanas in Argentina.

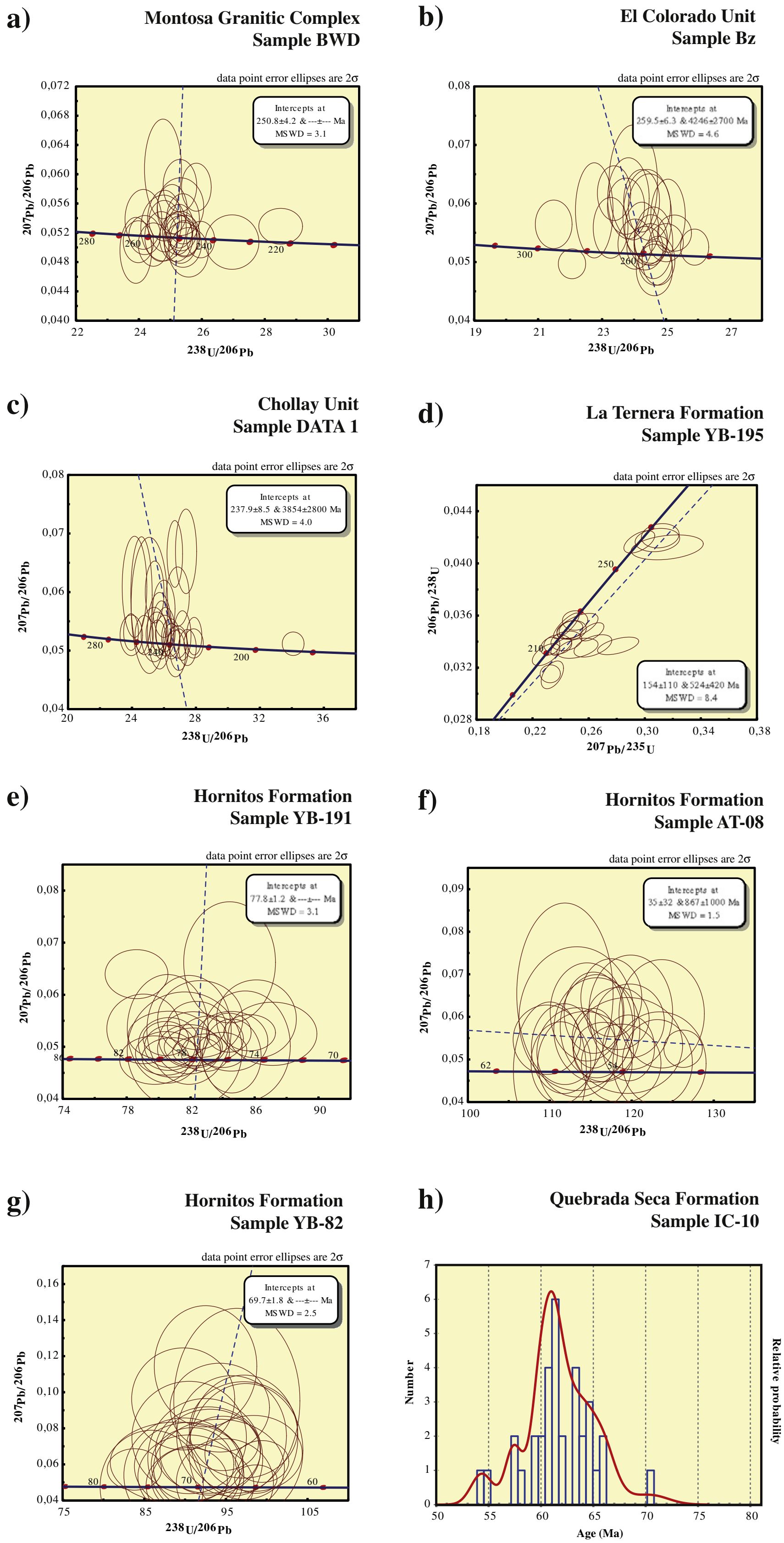

Fig. 17. a–g) Concordia plots of LA-ICPMS U–Pb analyses of zircons from the basement blocks (Montosa Granitic Complex), syn-rift deposits (La Ternera Formation), and synorogenic deposits (Hornitos Formation); h) U–Pb frequency plot ages from detrital zircons of the Quebrada Seca Formation.

2 Ma (DATA 1; Chollay Unit), 249.6 ± 1.1 Ma (BWD; Montosa Granitic Complex), and 259.3 ± 1.7 Ma (Bz; El Colorado Unit). These ages are younger than those determined previously using the K–Ar method (Farrar et al., 1970; Iriarte et al., 1999; Moscoso et al., 2010; Mpodozis and Kay, 1990; Zentilli, 1974), indicating that the Frontal Cordillera plutonic complex is Late Permian–Middle Triassic. A new U–Pb age of 213.2 ± 1.3 Ma (YB-195) was obtained from a lithic andesitic tuff corresponding to the syn-rift deposits of the La Ternera Formation, indicating that the age of this formation is Late Triassic (Figs. 2 and 17). To determine the age of the deformation, the ignimbrites and tuffs exposed in the lower and upper sections of the synorogenic Cenozoic deposits of the Hornitos and Quebrada Seca Formations were obtained. A new U–Pb age of 78.2 ± 0.6 Ma (YB-191) was obtained for the base of the Hornitos Formation on the footwall of the Calquis Fault. Similar and older ages (80 Ma) have been reported by Peña et al. (2013) for the western flank of the Hornitos Fold System and by Martínez et al. (2015) for the basement reverse faults located in the eastern Frontal Cordillera. Younger ages of 68.9 ± 1.5 Ma (YB-82) and 54.9 ± 0.5 Ma (AT-08) were determined for the intrusive bodies located along the fold axis, which could possibly have been emplaced through these structures (Figs. 2 and 17). A younger age of 60.5 ± 1.0 Ma (IC-10) was obtained for the upper section of the volcano-sedimentary deposits of the Quebrada Seca Formation, which are overthrust by the Vizcachas Fault along the eastern edge of the Montosa Horst (Figs. 2 and 16).

Based on all of the new data considered in this study, we concluded that Andean deformation started in the Late Cretaceous. This conclusion is supported by the angular unconformity between the 78-Ma synorogenic Hornitos Formation and the Triassic syn-rift deposits. Similar stratigraphic relationships were observed by Martínez et al. (2015) between Upper Cretaceous and lower Paleocene synorogenic deposits exposed along the basement-cored anticlines in the eastern Frontal Cordillera. Furthermore, the age of 60 Ma for the synorogenic deposits of the Quebrada Seca Formation suggests that deformation had migrated to the eastern Chilean Frontal Cordillera by that time. This last interpretation is confirmed by the Miocene ages of ~20.1 ± 0.9 Ma determined using the K–Ar method (Fig. 2) (Moscoso et al., 2010) for the volcanic and sedimentary deposits of the Doña Ana Formation, which unconformably overlies the Quebrada Seca Formation between the El Potro and Mondaquita faults. Based on the data and observations presented here, we propose that the growth of the orogenic belt in the flat-slab subduction segment (27–29°S) migrated eastward from the Late Cretaceous to the Miocene (Supplementary Data 2), although Andean deformation continues to occur toward the eastern side of the Frontal Cordillera, specifically, in the Sierras Pampeanas of Argentina.

7. Discussion

Like other flat-slab segments along the Andean Cordillera (such as the Bucaramanga and Peruvian flat-slab segments) (Ramos, 2009), the tectonic style above the flat-slab subduction segment in northern Chile is dominated mainly by thick-skinned deformation related to the tectonic inversion of former Mesozoic basins and the development of new thrust systems. For approximately three decades, the crustal structure of the flat-slab segment in northern Chile was interpreted as a set of basement blocks bounded by high-angle faults, comparable to those observed in other regions, such as the Sierra de Perijá in Colombia, the Venezuelan Mérida Andes, and the Laramide Belt of the western United States and Canada (Jordan and Allmendinger, 1986, 1983; Moscoso and Mpodozis, 1988; among others). However, our structural interpretation, which is based on field observations and geological mapping along the Mesozoic basins in northern Chile, shows the tectonic styles (e.g., inversion anticlines, short-cut faults, basement-cored folds, and basement thrust faults) that are the result of the tectonic inversion of Early Jurassic (Lautaro Basin)–Early Cretaceous (Chañarcillo Basin) half-grabens and the generation of new thrust systems.

This hybrid tectonic process (tectonic inversion and generation of new thrusts) has played a fundamental role in the growth of the orogenic belt and can be recognized in the Mesozoic basins mainly by the folding style of the thick syn-rift successions along their master faults. This folding style is characterized by long-wavelength eastward- and westward-vergent anticlines, interpreted as large-scale inversion anticlines, exposed in the eastern Coastal Cordillera and the western Frontal Cordillera, which define a doubly vergent fault system. Similar tectonic frameworks based on doubly vergent fault systems have been identified in neighboring regions (e.g., the Sierras Pampeanas and Bermejo Basin in Argentina and the Malargüe Thrust Fold Belt) from 2-D seismic profiles (Orts et al., 2012) and have been defined as a special type of thick-skinned triangle zone (Zapata and Allmendinger, 1996). In these regions, the compressional reactivation of normal faults, major suture zones, and mylonitic shear zones has formed thrust systems composed of doubly vergent thrusts and folds. The development of other thrust systems by tectonic inversion has also been suggested for the Salar de Atacama Basin and the Domeyko Cordillera in northern Chile, and it has been suggested that this development was associated with the closure of the Tarapacá Basin (Amilibia et al., 2008; Mpodozis et al., 2005).

In contrast to other regions located to the north of the flat-slab segment (e.g., the Subandean fold–thrust belt), the tectonic vergence along this segment is preferentially determined using the deformation ages only. Based on the age of the volcano-sedimentary synorogenic deposits, we suggest that compressional deformation started at approximately 78 Ma (Late Cretaceous) with the tectonic inversion of the Chañarcillo and Lautaro Basins and was followed by the eastward propagation of basement ramps during the Paleocene–Miocene times, some of which cut inherited basement highs. We further suggest that the crustal thickness in this region is a function of shortening along these large ramps (Fig. 16). In contrast, on the Argentinean side, the reactivation of suture zones that separate Paleozoic basement terranes related to ancient collisional episodes (Ramos et al., 2002) and the propagation of eastward and westward reverse-dipping faults are proposed to explain the uplift of large basement blocks exposed to the east of the Chilean Frontal Cordillera in the Sierras Pampeanas (Supplementary Data 2).

These results confirm that the Andean deformation in the Chilean Frontal Cordillera did not occur during the late Miocene–Pliocene, as suggested in previous studies (Moscoso and Mpodozis, 1988; Ramos et al., 2002), however, important reactivations were recorded by some structures in this region. The chronological record described for Andean deformation at this latitude (Supplementary Data 2) has also been determined from synorogenic deposits exposed in other thrust systems along the Andean Cordillera, such as: the Colombian Eastern Cordillera, the Marañon Basin in Peru, and the Salar de Atacama Basin in northern Chile (Arriagada et al., 2006; Cobbold et al., 2007; Mpodozis et al., 2005), however, recent analyses of exhumation timing carried out in the Neuquén Basin in Argentina also have indicated an important episode of Andean deformation during the Late Cretaceous (Balgord and Carrapa, 2014; Folguera et al., 2015), which is mainly associated with a rapid trenchward continental shifting (Semperé et al., 1997; Cobbold et al., 2007; Folguera et al., 2015). Because the older deformation is recorded in the Eastern Coastal Cordillera, we suggest that it represents the "main piston" that triggered the tectonic inversion of the intracontinental Mesozoic basins. Starting with this episode, the Andean deformation progressively migrated toward the east (e.g., the Sierras Pampeanas) where the crustal shortening was mainly accommodated by large reverse faults that uplifted huge basement blocks near the Chile–Argentina frontier (Ramos et al., 2002; Fig. 16b).

8. Conclusions

We conclude that the tectonic style recognized along the "Pampean" flat-slab subduction segment in northern Chile is dominated by the interaction of inverted structures and basement-involved compressive faults. The reactivation of former Mesozoic extensional master faults produced large NNE-striking asymmetric anticlines exposed along the Coastal Cordillera and Frontal Cordillera, forming a doubly vergent fault system. These findings confirm the premise that the tectonic styles observed in this region are mainly controlled by the region's previous crustal Mesozoic history, as in other regions of the Central Andes. On the other hand, the oldest ages of deformation determined here (~80 Ma) allowed us to propose that the Andean orogenesis in the "Pampean" flat-slab segment was initiated by tectonic inversion processes during the so-called "Peruvian" tectonic phase in the Coastal Cordillera and, which migrated progressively to the eastern sector during the Paleocene to Miocene time (~60–20 Ma). This evidence demonstrates that the age of the structure in this region is not purely Neogene and did not occur in a single compressive pulse as it was indicated by previous works. Even, there are recent data that point to a Late Cretaceous age for the initial growth of the Frontal Cordillera. The Paleocene to Miocene Andean deformation was characterized by eastward-vergent propagation of basement-involved reverse faults that uplifted inherent basement highs along the Frontal Cordillera. We suggest that this resulted in the largest crustal shortening (40.94 km) of this Andean segment. Finally, we suggest that inversion structures and doubly vergent fault systems can be expected to exist in other regions in northern Chile, especially in regions where former Mesozoic basins are present.

Supplementary data to this article can be found online at http://dx.doi.org/10.1016/j.tecto.2015.11.019.

Acknowledgments

This research was funded by the Fondo Nacional de Desarrollo Científico y Tecnológico (FONDECYT), Chile (grants 1050750, 1070964 and 3140557) and by the Institut de Recherche pour le Développent (IRD). Thanks to Midland Valley, who kindly provided us with the 2D MOVE software to perform part of this study. The authors acknowledge the valuable discussions with Dr. Constantino Mpodozis. We thank reviewers Victor Ramos and Andrés Folguera for their valuable and constructive comments on an earlier version of this manuscript. We would also like to thank Sergio Villagrán and Marco Vaccaris for their assistance in the field and J. Vargas and R. Valles (Geology Department, Universidad de Chile), for zircon sample preparation, as well as L. Solari for U–Pb LA-ICP-MS analyses (LEI, UNAM).

References

Aguirre-Urreta, B., 1993. Neocomian ammonite biostratigraphy of the Andean basins of Argentina and Chile. Rev. Española de Paleontología 8, 57–74.
Allmendinger, R., Figueroa, D., Snyder, D., Beer, J., Mpodozis, C., Isacks, B.L., 1990. Foreland shortening and crustal balancing in the Andes at 30°S latitude. Tectonics 9, 789–809.
Allmendinger, R.W., Jordan, T.E., Kay, S.M., Isacks, B.L., 1997. The evolution of the Altiplano–Puna Plateau of the central Andes. Annu. Rev. Earth Planet. Sci. 25, 139–174.
Alvarado, P., Ramos, V., 2011. Earthquake deformation in the northwestern Sierras Pampeanas of Argentina based on seismic waveform modelling. J. Geodyn. 51, 205–211.
Amilibia, A., Sàbat, F., McClay, K.R., Muñoz, J.A., Roca, E., Chong, G., 2008. The role of inherited tectono-sedimentary architecture in the development of the central Andean mountain belt: insights from the Cordillera de Domeyko. J. Struct. Geol. 30, 1520–1539.
Arévalo, C., 1994. Mapa geológico de la Hoja Los Loros, Región de Atacama (1:100.000). Servicio Nacional de Geología y Minería, Documentos de, Trabajo No#6.
Arévalo, C., 1999. The Coastal Cordillera–Precordillera boundary in the Copiapó area, northern Chile, and the structural setting of the Candelaria Cu–Au ore deposit. Unpublished Ph.D. Thesis. Kingston University, Kingston-upon-Thames, UK, 244 p.
Arévalo, C., 2005a. Carta Copiapó, Región de Atacama. Servicio Nacional de Geología y Minería, Carta Geológica de Chile, Santiago. 91, 54 p, scale: 1:100.000.
Arévalo, C., 2005b. Carta los Loros, Región de Atacama, Carta Geológica Básica. Servicio Nacional de Geología y Minería, Santiago. 92, 54 p, scale: 1:100.000.
Arévalo, C., Welkner, D., 2008. Carta Carrizal Bajo-Chacritas, Región de Atacama, Carta Geológica Básica. Servicio Nacional de Geología y Minería, Santiago, scale: 1:100.000.
Arriagada, C., Cobbold, P., Roperch, P., 2006. Salar de Atacama basin: a record of compressional tectonics in the central Andes since the mid-Cretaceous. Tectonics 25, 1–19.
Arriagada, C., Roperch, P., Mpodozis, C., Cobbold, P.R., 2008. Paleogene building of the Bolivian Orocline: tectonic restoration of the central Andes in 2-D map view. Tectonics 27, 1–14.
Arriagada, C., Ferrando, R., Córdova, L., Morata, D., Roperch, P., 2013. The Maipo Orocline: a first scale structural feature in the Miocene to Recent geodynamic evolution in the central Chilean Andes. Andean Geol. 4 (3), 419–437.
Bahlburg, H., Breitkreuz, C., 1993. Differential response of Devonian–Carboniferous platform-deeper basin system to sea-level change and tectonics, N. Chilean Andes. Basin Res. 5, 21–40.
Balgord, E., Carrapa, B., 2014. Basin evolution of Upper Cretaceous–Lower Cenozoic strata in the Malargüe fold-and-thrust belt: northern Neuquén Basin, Argentina. Basin Res. 1–24. http://dx.doi.org/10.1111/bre.12106.
Baraganzi, M., Isacks, B.L., 1976. Spatial distribution of earthquakes and subduction of the Nazca plate beneath South America. Geology 4, 686–692.
Bascuñan, S., Arriagada, C., Le Roux, J., Deckart, K., 2015. Unraveling the Peruvian Phase of the Central Andes: stratigraphy, sedimentology and geochronology of the Salar de Atacama Basin (22°30–23°S), norther Chile. Basin Res. http://dx.doi.org/10.1111/bre.12114.
Bell, C.M., 1984. Deformation produced by the subduction of a Paleozoic turbidite sequence in northern Chile. J. Geol. Soc. 141, 339–347.
Bevis, M., Isacks, B., 1984. Hypocentral trend surface analysis: probing the geometry of Benioff zones. J. Geophys. Res. 89, 6153–6170.
Brown, M., Diaz, F., Grocott, J., 1993. Displacement history of the Atacama Fault System 25°00′–27°00′ S, northern Chile. Geol. Soc. Am. Bull. 105, 1165–1174.
Cahill, T., Isacks, B.L., 1992. Seismicity and shape of the subducted Nazca Plate. J. Geophys. Res. 97 (17), 503–529.
Carrapa, B., Trimble, J.D., Stockli, D., 2011. Patterns and timing of exhumation and deformation in the Eastern Cordillera of NW Argentina revealed by (U–Th)/He thermochronology. Tectonics 30, 1–30.
Carrera, N., Muñoz, J.A., Sàbat, F., Roca, E., Mon, R., 2006. The role of inversion tectonics in the structure of the Cordillera Oriental (NW Argentinean Andes). J. Struct. Geol. 28, 1921–1932.
Charrier, R., 1979. El Triásico en Chile y regiones adyacentes de Argentina: Una reconstrucción paleogeográfica y paleoclimática. Comunicaciones 26, 1–47.
Charrier, R., Pinto, L., Rodríguez, M.P., 2007. Tectonostratigraphic evolution of the Andean Orogen in Chile. In: Moreno, T., Gibbons, W. (Eds.), The Geology of Chile. The Geological Society, London, pp. 21–114.
Charrier, R., Hérail, G., Pinto, L., García, M., Riquelme, R., Farías, M., Muñoz, M., 2013. Cenozoic tectonic evolution in the Central Andes in northern Chile and west-central Bolivia. Implications for paleogeographic, magmatic and mountain building evolution. Int. J. Earth Sci. 102, 235–264.
Cobbold, P.R., Rossello, E.A., Roperch, P., Arriagada, C., Gómez, L.A., Lima, C., 2007. Distribution and timing of Andean deformation across South America, in Global Tectonic Processes: The legacy of Mike Coward, edited by A. Ries, R. H. Graham, and R. W. Butler. Geol. Soc. Spec. Publ.
Cornejo, P., Mpodozis, C., Ramírez, C., Tomlinson, A., 1993. Estudio geológico de la Región de Potrerillos y El Salvador (26°–27° Lat. S), Reg. Rep. IR-93-01, 2. Servicio Nacional de Geología y Minería. 12, scale: 1:50.000.
Coutand, I., Cobbold, P., Urreiztieta, M., Gautier, P., Chauvin, A., Gapais, D., Rossello, E., Gamundi, O., 2001. Style and history of Andean deformation, Puna plateau, northwestern Argentina. Tectonics 20, 210–234.
Dallmeyer, D.R., Brown, M., Grocott, J., Graeme, T.K., Treloar, P.J., 1996. Mesozoic magmatic and tectonic events within the Andean Plate Boundary Zone, 26°–27°30′S, North Chile: constraints from $^{40}Ar/^{39}Ar$ Mineral Ages. J. Geol. 104, 19–40.
DeCelles, P.G., Carrapa, B., Horton, B.K., Gehrels, G.E., 2011. Cenozoic foreland basin system in the central Andes of northwestern Argentina: implications for Andean geodynamics and modes of deformation. Tectonics 30, 1–30.
Farrar, E., Clark, A.H., Haynes, S.J., Quirt, G., Conn, H., Zentilli, M., 1970. K–Ar evidences for the post-Paleozoic migration of magmatic foci in the Andes of northern Chile. Earth Planet. Sci. Lett. 10, 60–66.
Folguera, A., Bottesi, G., Duddy, I., Martín-Gonzalez Orts, D., Sagripanti, L., Vera, Rojas, Ramos, V.A., 2015. Exhumation of the Neuquén Basin in southern Central Andes (Malargüe fold and thrust belt) from field data and low-temperature thermochronology. J. S. Am. Earth Sci. 1–18 (xxx).
Franzese, J.R., Spalletti, L.A., 2001. Late Triassic–early Jurassic continental extension in southwestern Gondwana: tectonic segmentation and pre-break-up rifting. J. S. Am. Earth Sci. 14, 257–270.
Godoy, E., Davidson, J.D., 1976. Pilares en compresión de edad Mioceno superior en los Andes del Norte de Chile (22°–30° Latitud Sur), paper presented at I Congreso Geológico Chileno. 1, pp. 87–103.
Grier, M.E., Saltity, J.A., Allmendinger, R.W., 1991. Andean reactivation of the Cretaceous Salta rift, northwestern Argentina. J. S. Am. Earth Sci. 4 (4), 351–372.
Grocott, J., Taylor, G., 2002. Magmatic arc fault systems, deformation partitioning and emplacement of granitic complexes in the Coastal Cordillera, north Chilean Andes (25°30′ to 27°00′S). J. Geol. Soc. Lond. 159, 425–442.
Iaffa, D., Sàbat, F., Muñoz, J.A., Mon, R., Gutierrez, A.A., 2011. The role of inherited structures in a foreland basin evolution. The Metán Basin in NW Argentina. J. Struct. Geol. 33, 1816–1828.
Iriarte, S., Arévalo, A., Mpodozis, C., 1999. Hoja La Guardia, Región de Atacama. Servicio Nacional de Geología y Minería, Santiago, escala 1:100.000
Isacks, B.L., 1988. Uplift of the Central Andes Plateau and bending of the Bolivian Orocline. J. Geophys. Res. 93, 3211–3231.
Jensen, O., 1976. Geología de las nacientes del río Copiapó, entre los 27°53′ y 28°20′ de latitud Sur, provincia de Atacama. Memoria de Titulo (Inédito), Universidad de Chile, Departamento de Geología, Chile (249 pp.).
Jensen, O., Vicente, J.C., 1976. Estudio geológico del área de "Las Juntas" del rio Copiapó (Provincia de Atacama-Chile). Rev. Asoc. Geol. Argent. 21, 145–173.

Jordan, T., Allmendinger, R., 1986. The Sierras Pampeanas of Argentina: a modern analogue of Rocky Mountain foreland deformation. Am. J. Sci. 286, 737–764.

Jordan, T., Isacks, B.L., Allmendinger, R., Brewer, J., Ramos, V., Ando, C., 1983. Andean tectonics related to geometry of subducted Nazca plate. Geol. Soc. Am. Bull. 94, 341–361.

Kley, J., Monaldi, C.R., 1998. Tectonic shortening and crustal thickness in the Central Andes: how good is the correlation? Geology 26, 723–726.

Kley, J., Monaldi, C.R., Salfity, J.A., 1999. Along-strike segmentation of the Andean foreland: causes and consequences. Tectonophysics 301, 75–94.

Lara, L and Godoy, E., 1998. Mapa Geológico de la Hoja Quebrada Salitrosa, Región de Atacama. Servicio Nacional de Geología y Minería, Santiago, scale: 1:100.000

Ludwing, K.R., 2008. Isoplot 3.6. 4. Berkley Geochronology Center Special, Publication.

Maksaev, V., Munizaga, F., Valencia, V., Barra, F., 2009. LA-ICP-MS zircón U–Pb geochronology to constrain the age of post-Neocomian continental deposits of the Cerrillos Formation, Atacama Region, northern Chile: tectonic and metallogenic implications. Andean Geol. 36, 264–287.

Marschik, R., Fontboté, L., 2001. The Candelaria–Punta del Cobre iron oxide Cu–Au (–Zn–Ag) deposits, Chile. Econ. Geol. 96, 1799–1826.

Martin, M., Clavero, R., Mpodozis, C., 1997. Eocene to late Miocene magmatic development of El Indio belt, 30°S, North Central Chile, paper presented at VIII° Congreso Geológico Chileno. 1 pp. 149–153 (Antofagasta).

Martínez, F., Arriagada, C., Mpodozis, C., Peña, M., 2012. The Lautaro Basin: a record of inversion tectonics in northern Chile. Andean Geol. 39 (2), 258–278.

Martínez, F., Arriagada, C., Peña, M., Del Real, I., Deckart, K., 2013. The structure of the Chañarcillo Basin: an example of tectonic inversion in the Atacama region, northern Chile. J. S. Am. Earth Sci. 42, 1–16.

Martínez, F., Arriagada, C., Valdivia, R., Deckart, K., Peña, M., 2015. Geometry and kinematics of the Andean thick-skinned thrust systems: insights from the Chilean Frontal Cordillera (28°–28.5°S), Central Andes. J. S. Am. Earth Sci. 1–18 (xxx).

Mortimer, C., 1973. The Cenozoic history of the southern Atacama Desert, Chile. J. Geol. Soc. Lond. 129, 505–526.

Moscoso, R., Mpodozis, C., 1988. Estilos estructurales en el Norte Chico de Chile (28°–31°S), regiones de Atacama y Coquimbo. Rev. Geol. Chile 15, 155–158.

Moscoso, R., Mpodozis, C., Nassi, C., Ribba, L., Arévalo, C (Compilador)., 2010. Geología de la Hoja El Tránsito, Región de Atacama. Servicio Nacional de Geología y Minería de Chile, Serie Preliminar, 7, scale: 1:250.000, 3 anexos, Santiago.

Mourgues, F.A., 2004. Advances in ammonite biostratigraphy of the marine Atacama basin (Lower Cretaceous), northern Chile, and its relationship with the Neuquén basin, Argentina. J. S. Am. Earth Sci. 17, 3–10.

Mpodozis, C., Cornejo, P., 1997. El rift Triásico- Sinemuriano de Sierra Exploradora, Cordillera de Domeyko (25°–26°S): Asociaciones de facies y reconstrucción tectónica, paper presented at VIII Congreso Geológico Chileno. 1 pp. 550–554.

Mpodozis, C., Kay, S., 1990. Provincias magmáticas ácidas y evolución tectónica de Gondwana: Andes chilenos (28–31°S). Rev. Geol. Chile 17, 153–180.

Mpodozis, C., Ramos, V., 1990. The Andes of Chile and Argentina. In: Ericksen, G.E., Cañas Pinochet, M.T., Reinemud, J.A. (Eds.), Geology of the Andes and its relation to hydrocarbon and mineral resources: Circumpacific Council for Energy and Mineral Resources. Earth Science Series 11, pp. 59–90.

Mpodozis, C., Ramos, V.A., 2008. Tectónica jurásica en Argentina y Chile: Extensión, Subducción Oblicua, Rifting, Deriva y Colisiones? Rev. Geol. Argent. 63, 479–495.

Mpodozis, C., Arriagada, C., Basso, M., Pierrick, R., Cobbold, P., Reich, M., 2005. Late Mesozoic to Paleogene stratigraphy of the Salar de Atacama Basin, Antofagasta, Northern Chile: implications for the tectonic evolution of the Central Andes. Tectonophysics 399, 125–154.

Naranjo, J.A., Puig, A., 1984. Hojas Taltal y Chañaral, Regiones de Antofagasta y Atacama. Servicio Nacional de Geología y Minería, Santiago, pp. 62–63 (140 pp.).

Oliveros, V., Féraud, G., Aguirre, L., Fornari, M., Morata, D., 2006. The Early Andean Magmatic Province (EAMP): $^{40}Ar/^{39}Ar$ dating on Mesozoic volcanic and plutonio rocks from the Coastal Cordillera, Northern Chile. J. Volcanol. Geotherm. Res. 157, 311–330.

Oliveros, V., Labbé, M., Rossel, P., Charrier, R., Encinas, A., 2013. Late Jurassic paleogeographic evolution of the Andean back-arc basin: new constrains from the Lagunillas Formation, northern Chile (27°30′–28°30′S). J. S. Am. Earth Sci. 37, 25–40.

Orts, D., Folguera, A., Giménez, M., Ramos, V., 2012. Variable structural controls through time in the Southern Central Andes (~36°S). Andean Geol. 39 (2), 220–241.

Peña, M., Arraigada, C., Mpodozis, C., Martínez, F., Salazar, E., 2010. Rotaciones tectónicas sobreimpuestas en la zona centro-sur de la Región de Atacama: Primeros resultados de un estudio estructural y paleomagnético, paper presented at XII Congreso Geológico Chileno.

Peña, M., Arriagada, C., Martínez, F., Becerra, J., 2013. Carta Geológica Yerbas Buenas-Tres Morros, Región de Atacama. Servicio Nacional de Geología y Minería, Santiago, scale: 1:100.000.

Pindell, J., Dewey, J., 1982. Permo-Triassic reconstruction of western Pangea and the evolution of the Gulf of Mexico/Caribbean region. Tectonics 1, 179–211.

Price, G., Dashwood, B., Taylor, G., Kalin, M., Ogle, N., 2008. Carbon isotope and magnetostratigraphy of the Cretaceous (Barremian and Aptian) Pabellón Formation, Chañarcillo Basin, Chile. Cretac. Res. 29, 183–191.

Ramos, V.A., 2009. Anatomy and global context of the Andes: main geologic features and the Andean orogenic cycle. In: Kay, S.M., Ramos, V.A., Dickinson, W.R. (Eds.), Backbone of the Americas: shallow subduction, plateau uplift, and ridge and terrane collision. The Geological Society of America. Memoir 204, pp. 31–65.

Ramos, V.A., Cristallini, E.O., Pérez, D.J., 2002. The Pampean flat-slab of the Central Andes. J. S. Am. Earth Sci. 15, 59–78.

Reutter, K.J., 1974. Entwicklung und Bauplan der chilenischen Hochkordillere im Bereich 29° südlicher Breite. N. Jb. Geol. Paläont. 146, 153–178.

Rodríguez, M.P., 2013. Cenozoic uplift and exhumation above the southern part of the flat slab subduction segment of Chile (28.5–32°S). Unpublished Ph.D. Thesis. University of Chile, Santiago, 181 p.

Scheubert, E., Reutter, K.J., 1992. Magmatic arc tectonics in the Central Andes between 21° and 25°S. Tectonophysics 205, 127–140.

Segerstrom, K., 1960. Cuadrángulo Quebrada Paipote, Provincia de Atacama, Carta Geológica de Chile. Instituto de Investigaciones Geológicas, Santiago de Chile (35 pp.).

Segerstrom, K., Ruiz, C., 1962. Cuadrángulo Copiapó, Provincia de Atacama, Carta Geológica de Chile. 6. Instituto de Investigaciones Geológicas, Santiago de Chile (115 pp.).

Segerstron, K., Parker, 1959. Cuadrángulo Los Loros, Provincia Atacama, Carta Geológica de Chile. Instituto de Investigaciones Geológicas, Santiago de Chile (33 pp.).

Semperé, T., Butler, R.F., Richards, D.R., Marshall, L.G., Sharp, W., Swisher III, C.C., 1997. Stratigraphy and chronology of Upper Cretaceous–lower Paleogene strata in Bolivia and northwest Argentina. Geol. Soc. Am. Bull. 109, 709–727.

Sepúlveda, P., Naranjo, J. A., 1982. Hoja Carrera Pinto, Región de Atacama. Servicio Nacional de Geología y Minería, Santiago, 53, 62 p, scale: 1:100.000.

Soffia, J.M., 1989. Estratigrafía y geología estructural del área del río Jorquera, Región de Copiapó. Memoria de Título (Inédito). Universidad de Chile, Departamento de Geología (159 pp.).

Solari, L.A., Gómez-Tuena, A., Bernal, J.P., Pérez-Arvizu, O., Tanner, M., 2010. U–Pb zircón geochronology by an integrated LAICPMS microanalytical workstation: achievements in precision and accuracy. Geostand. Geoanal. Res. 34 (1), 5–18.

Somoza, R., 1998. Updated Nazca (Farallon)–South America relative motions during the last 40 My: implications for mountain building in the central Andean region. J. S. Am. Earth Sci. 11, 211–215.

Steinman, G., 1929. Geologie von Peru. Carl Winters Universitats-Buchhandlung (448 pp.).

Suárez, M., Bell, C.M., 1992. Triassic rift-related sedimentary basins in northern Chile (24°–29° S). J. S. Am. Earth Sci. 6, 109–121.

Taylor, G., Grocott, J., Pope, A., Randall, D., 1998. Mesozoic fault systems, deformation and fault block rotation in the Andean forearc: a crustal scale strike-slip duplex in the Coastal Cordillera of Northern Chile. Tectonophysics 299, 93–109.

Taylor, G., Grocott, J., Dashwood, B., Gipson, M., Arévalo, C., 2007. Implications for crustal rotation and tectonic evolution in the central Andes forearc: new paleomagnetic results from the Copiapó region of northern Chile, 26°–28°S. J. Geophys. Res. 112. http://dx.doi.org/10.1029/2005JB003950.

Thiele, R., 1964. Reconocimiento geológico de la Alta Cordillera de Elqui, Universidad de Chile, Departamento de Geología. 27. Publicaciones, pp. 1–73.

Willis, B., 1929. Earthquake conditions in Chile. Carnegie Inst. Publ. 382 (178 pp.).

Yamada, Y., McClay, K., 2003. Application of geometric models to inverted listric fault systems in sandbox experiments. Paper 1: 2D hanging wall deformation and section restoration. J. Struct. Geol. 25, 1551–1560.

Zapata, T., Allmendinger, R., 1996. Thrust–front zone of the Precordillera, Argentina; a thick-skinned triangle zone. A.A.P.G Bull. 80, 359–381.

Zentilli, M., 1974 Geological evolution and metallogenic relationships in the Andes of N. Chile. PhD Thesis (Unpublished), Queen's University, Canada, 446 p.